Original Research Article   **Open Access Journal**

N-Substituted (substituted-5-benzylidine) thiazolidine-2,4-diones:Crystal structure, In Silico, DNA binding and anticancer studies

Imran Ali [*, 1], Mohammad Nadeem Lone [1], Ming-Fa Hsieh [2]

[1]Department of Chemistry, Jamia Millia Islamia (Central University), New Delhi-110025, India
[2]Department of Biomedical Engineering, Chung Yuan Christian University, 200, Chung Pei Rd., Chung Li, Taiwan

*corresponding author e-mail address:*drimran_ali@yahoo.com; drimran.chiral@gmail.com*

ABSTRACT

The development of efficient anticancer agents is in a continuing chase by medicinal chemists. The present work reports the syntheses, characterization, X-ray crystal analysis, DNA binding, anticancer activities, DNA docking and Lipkinsin's rule studies of N-substituted (substituted-5-benzylidine) thiazolidine-2,4-diones. All the compounds were stable in PBS at pH 7.4 for 36 h. The structures of compounds have been determined by ^{1}H NMR, ^{13}C NMR, IR and X-ray analysis. The values of DNA binding constants of the compounds ranged from 7.07×10^2 to 2.50×10^8 M^{-1}. The spectrophotometric data and the simulation studies indicated that most of the compounds interacted with DNA *via* minor groves. The docking affinities of the compounds varied from 5.4-6.6 kcal/mol. The binding among the compounds and DNA was observed to be due to hydrogen bondings and hydrophobic interactions. The compounds formed 1 to 4 hydrogen bonds with the nucleobases of DNA. Some compounds showed marked activities (~46.17%) with IC$_{50}$ values in low micromolar range. Interestingly, all the studies carried out were in good agreement with each other. Overall, the reported compounds demonstrated interesting pharmacological properties. These molecules may be future drugs for liver cancer treatment.

Keywords: *N-Substituted Thiazolidine-2,4-Diones, DNA Binding, Solution Stabilities, Molecular Docking and Anticancer Activities, X-ray Analysis.*

1. INTRODUCTION

Cancer is the leading cause of death in individuals aged below 85 years in United States [1]. About, 100 different types of cancers have been reported globally. The number is expected to increase by 2025. Approximately, 72 billion US $ are spent annually in USA for the treatment of cancer [2]. In spite of many chemotherapeutic strategies for cancer treatment, this disease remains tenacious and deadly.

The different heterocyclic compounds have been explored on various cancer cell lines [3, 4]. Out of the huge and diverse pool of heterocyclic compounds investigated on different cancer cell lines, many compounds have showed inhibition of cancer cells [5]. Some naturally occurring and synthetic heterocyclic anticancer drugs (paclitaxel, anastrozole, zoledronic acid, irinotecan, etc.) are available in market for the treatment of lung, breast, prostate, leukemia, etc.

However, it has been established that these drugs unable to cure cancers completely; especially at chronic and late stages. Besides, certain serious side effects further limit their applications. In view of these facts, there is an urgent need to develop efficient and safe heterocyclic compounds for overcoming the threats posed by different cancers.

Thiazolidine-2,4-dione (TZD) moiety has been the centre of interest in medicinal organic chemistry in the present scenario. It is due to its anticancer, antibacterial, antifungal, antiviral, anti-tuberculosis, anti-parasitic and anti-microbial activities [6-9].

Furthermore, TZD has been found effective against multiple cancers including prostate, colon, breast, lung, stomach, etc. [10-13]. Therefore, TZD and other related heterocyclic moieties have been recognized as promising templates in anticancer drug designs strategies [14-19].

In view of these facts, attempts were made to synthesize Knoevenagel's condensates from promising moiety (TZD) and N-substituted thiazolidine-2,4-dione derivatives through substitution reactions of Knoevenagel's condensates (Table 1). The synthesized compounds were characterized by analytical and spectroscopic methods.

The solution stability, DNA binding and lactate based dehydrogenase cytotoxicity on HepG2 (human liver cancer cell line) were carried out. Furthermore, the crystal of one N-substituted compound [(5Z)-5-[(4-flurophenyl) methylidine]-3-propyl-1,3-thiazolidine-2,4] (3H) has been developed in hexane solution under normal conditions and its single crystal X-ray analysis is reported in the present paper.

Additionally, the simulation studies were also performed to determine the binding of the developed heterocyclic compounds with DNA. Finally, the mechanisms of action (interactions with DNA grooves) at a supramolecular level were developed using the data of the above studies. The results of these findings are reportedherein**.**

Table 1. Synthesized heterocyclic compounds (**3A-3R**) containing the basic framework of thiazolidine-2,4-dione.

Compounds	R	R$_1$	Compounds	R	R$_1$
3A	Cl	H	**3J**	F	-CH$_3$
3B	F	H	**3K**	F	-CH$_2$(C$_6$H$_5$)
3C	-OCH$_3$	H	**3L**	-OCH$_3$	-CH$_2$CH$_2$CH$_2$CH$_3$
3D	-NO$_2$	H	**3M**	-NO$_2$	-CH$_2$CH$_2$CH$_2$CH$_3$
3E	-CH$_3$	H	**3N**	-NO$_2$	-CH(CH$_3$)$_2$
3F	Cl	-CH$_2$CH$_2$CH$_2$CH$_3$	**3O**	-NO$_2$	-CH$_3$
3G	Cl	-CH(CH$_3$)$_2$	**3P**	-NO$_2$	-CH$_2$(C$_6$H$_5$)
3H	F	-CH$_2$CH$_2$CH$_3$	**3Q**	-CH$_3$	-CH$_2$CH$_2$CH$_2$CH$_3$
3I	F	-CH(CH$_3$)$_2$	**3R**	-CH$_3$	-CH(CH$_3$)$_2$

2. EXPERIMENTAL SECTION

2.1. Chemistry.

All the reagents were of A.R. grade and used without further purification. Methanol, ethyl acetate, chloroform, petroleum ether and hexane were of HPLC grade and procured from E. Merck, Mumbai, India. Thiourea, chloroacetic acid, *p*-chloro- benzaldehyde, *p*-nitrobenzaldehyde, *p*-methyl benzaldehyde, *p*-fluoro benzaldehyde, *p*-methoxy benzaldehyde, *m*-bromo benzaldehyde, *n*-butyl bromide, *n*-propyl bromide, isopropyl bromide, methyl bromide, benzyl choloride and sodium hydride were purchased from Spectrochem, Mumbai, India. Acetic acid and sodium acetate were supplied by Qualigens Fine Chemicals, Mumbai, India. The disodium salts of Ct-DNA were supplied from S.D. Fine Chem. Ltd, New Delhi, India. Pre-coated aluminum silica gel 60 F$_{254}$ thin layer plates were purchased from E. Merck, Germany. Human liver cancer cell lines (Hep G2) were collected from School of Pharmacy, College of Medicine, National Taiwan University. 3-(4,5-Dimethylthiazol-2-yl)-2,5-diphenyl tetrazolium bromide (MTT) was purchased from Sigma-Aldrich, St. Louis, MO, USA. Dulbecco's modified Eagle's medium (DMEM) and antibiotics/antimycotics were purchased from GIBCO NY, USA.

The bovine fetal serum (FBS) was obtained from HyClone, Utah, USA. LDH cytotoxicity detection kit (Takara, cat. no. MK401, Japanese) was used for the cytotoxicity tests. LDH released from the cells was detected by ELISA plate reader (Thermo, Multiskan™ FC, United State) at a wavelength of 490 nm. Untreated culture medium and 1% trion X-100 (Sigma, United State) were used as negative and positive controls, respectively. Student's t-test was used to determine the statistical significance ($p < 0.05$, $p < 0.01$ or $p < 0.001$).

The percentages of C, H, N, and S were determined by a Vario elemental analyzer (EL-III). UV–Vis spectra were obtained with a Perkin-Elmer Lambda 40 UV-Vis. spectrometer (CT 06859 USA). FT-IR spectra were recorded on a Perkin ElmerRXIFT system spectrometer (LR 64912C). ^{1}H NMR spectra were recorded using Bruker 400 MHz instrument (DPX 300). ESI-mass spectra were recorded with micrOTOF-Q II spectrometer (10262).

UV cabinet was used to view TLC plates. A pH meter of Control Dynamics (APX 175 E/C) was used to record pH of the solutions. The melting points were determined on Veegoinstrument (REC-22038 A2).

Millipore water was prepared using a Millipore Milli-Q (Bedford, MA, USA) water purification system. In silico studies were performed by AutoDock 4.2 Vina (Scripps Research Institute, USA) on Intel® core™ i3 CPU (3.2 GHz) with Windows XP operating system. Incubator for cell culture (MCO-15AC, Sanyo), centrifuge (CN 2060, Hsiangtai Co) and microplate photometer (Multiskan FC, Thermo Scientific) were used for carrying out the anticancer assays of the developed compounds.

2.2. Synthesis of thiazolidine-2,4-dione(2A).

An aqueous solution (15 mL) of chloroacetic acid (14.175 g; 0.150 M) was placed in a 100 mL round bottom flask. To this solution, 11.418 g (0.150 M) of thiourea were added with continuous stirring for 20 min. The reaction mixture was refluxed for 40 h at 100-110°C. On cooling, the contents of flask solidified into a white needle-like product. The solidified product was filtered and washed with sufficient amount of water to remove untreated substrates. It was dried and recrystallized with methanol to get pure thiazolidine-2,4-dione (2A). The schematic representation of the synthesis of 2A is given in Scheme 1.

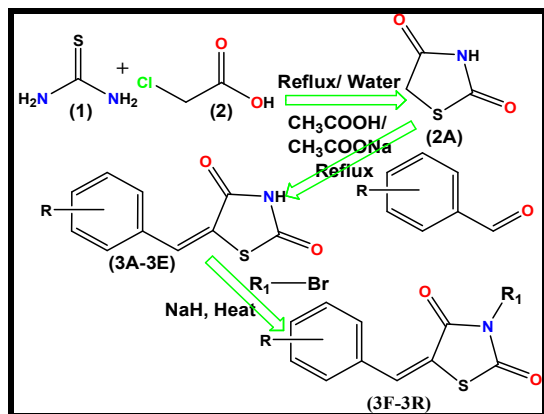## 2.3. Thiazolidine-2,4-dione (2A).

Yield: 85.0%, mol. wt 117.12 Da, mp 126-127 °C; Anal. Calcd: C (30.76%), H (2.58%), N (11.96%), O (27.32%), S (27.38%); found: C (30.75%), H (2.59%), N (11.96%), O (27.31%), S (27.37%); I.R.(KBr pellets, cm^{-1}): 3386.14 (υN-H)str, 1732.75 (υC=O)sym; ESI-MS (*m/z*) Calcd for C$_3$H$_3$NO$_2$S: 117.126, [M+Na-2H]$^+$, found: 115.7.

2.4. Synthesis of Substituted (5-benzylidine)-thiazolidine-2, 4-dione compounds (3A-3E)

A stirred solution of thiazolidine-2,4-dione (1.05 g, 9 mM) in 20.0 mL glacial acetic acid was buffered with sodium acetate (1.476 g, 18 mM). This was followed by the addition of substituted benzaldehydes (9 mM) for Knoevenagel's condensation. The resulting mixtures were refluxed with stirring

for 6 h. The completion of reactions was confirmed by TLC (petroleum ether-ethylacetate, 75:25, v/v). The final reaction mixtures were poured into ice-cold water, which resulted in the precipitation of the products (3A-3E).

The precipitates were filtered through a Buchner funnel and thoroughly washed with cold water. Finally, recrystallization was achieved with methanol, and the recrystallized products were dried in a vacuum dessicator over fused calcium chloride. The schematic representation of the syntheses of 3A-3E is given in Scheme 1.

Scheme 1. Synthesis of N-substituted (substituted 5-benzylidine)-thiazolidine-2,4-diones [2A- 3R].

2.5. 5-[(chlorophenyl)methylidine]-thiazolidine-2,4-dione (3A).

Yield: 80%, mp 153-155 °C, Anal. Calcd: C (50.11%), H (2.52%), Cl (14.79%), N (5.84%), O (13.35%), S (13.38%), found C (50.12%), H (2.52%), Cl (14.80%), N (5.83%), O (13.34%), S (13.36%); I.R. (KBr pellets, cm^{-1}): 3375.31 (υN-H)str, 3042.49 (υC-H aromatics) 1681.00 (υC=O)sym, 1573.48 (υCH=C). ^{1}H NMR (400 MHz, DMSO-d$_6$) δ (ppm): 7.93(s, 1H, CH=C), 7.58-7.52(m, 4H, Ar-H); ESI-MS (m/z) Calcd for C$_{10}$H$_6$ClNO$_2$S: [M+Na]$^+$, 239.68, found: 239.

2.6. 5-[(4-flurophenyl)methylidine]-thiazolidine-2,4-dione (3B).

Yield: 85.0%, mp 167-169 °C, Anal. Calcd: C (53.81%), H (2.71%), F (8.51%), N (6.27%), O (14.33%), S (14.36%), found C (53.80%), H (2.73%), F (8.52%), N (6.28%), O (14.31%), S (14.34%). I.R. (KBr pellets, cm^{-1}): 3471.80 (υN-H)str, 3102.65 (υC-H aromatics), 1725.68 (υC=O)sym. 1565.94 (υCH=C), 1283.33 (vC-S-C). ^{1}H NMR (400 MHz, DMSO-d6) δ (ppm): 7.41(s, 1H, CH=C), 7.61-7.27(m, 4H, Ar H). ESI-MS (m/z) Calcd for C$_{10}$H$_6$FNO$_2$S, 225.24, [M+Na+4H]$^+$,found: 239.

2.7. 5-[(4-methoxyphenyl)methylidine]-thiazolidine-2,4-dione (3C).

Yield: 80.0%, mp 188-190 °C; Anal. Calcd: C (56.16%), H (3.86%), N (5.95%), O (20.4%), S (13.63%), found C (56.17%), H (3.87%), N (5.97%), O (20.3%), S (13.65%). I.R. (KBr pellets, cm^{-1}): 1700.57 (υC=O)sym, 1500.40 (υCH=C), 1220.96 (υC-S-C); ^{1}H NMR (400 MHz, DMSO-d$_6$) δ (ppm): 7.75(s, 1H, -CH=C), 7.18-7.00(m, 4H, Ar-H), 3.79 (s, 3H, -OCH$_3$); ESI-MS (m/z) Calcd for C$_{11}$H$_9$NO$_3$S: 235, [M+Na+4H]$^+$,found: 239.

2.8.5-(4- nitrophenyl)methylidine)-thiazolidine-2,4-dione (3D).

Yield: 80%, mp 250-252ºC, Anal. Calcd: C (48%), H (2.42%), N (11.2%), O (25.58%), S (12.81%) found Anal. Calcd: C (48%), H (2.45%), N (11.4%), O (25.59%), S (12.85%); I.R. (KBr pellets, cm^{-1}): 3377.24 (υN-H)str, 3108.56 (υC-H aromatics), 1748.28 (υC=O)sym, 1571.38 (υCH=C), 1196.40 (υC-S-C); ^{1}H NMR (400 MHz, DMSO-d$_6$) δ (ppm): 13.01(s, 1H, -NH-), 7.95(s, 1H, -CH=C), 7.58-7.48(m, 4H, Ar-H).ESI-MS (m/z) Calcd for C$_{10}$H$_6$N$_2$O$_4$S [M+Na]$^+$: 250.232, found: 250.

2.9.5-[(4-methylphenyl)methylidine]-thiazolidine-2,4-dione (3E).

Yield: 85%, mp 195-198ºC, Anal. Calcd: C (60.26%), H (4.14%), N (6.39%), O (14.59%), S (14.62%), found C (60.27%), H (4.15%), N (6.38%), O (14.58%), S (14.63%); I.R. (KBr pellets, cm^{-1}): 3100.00 (υC-H aromatics), 1690 (υC=O)sym, 1550 (υCH=C), 1310.40 (υC-S-C).^{1}H NMR (400 MHz, DMSO-d$_6$) δ (ppm): 7.25(s, 1H, -CH=C), 7.28-7.15(m, 4H, Ar-H), 2.35 (s, 3H, Ar- CH$_3$); ESI-MS (m/z) Calcd for C$_{11}$H$_9$NO$_2$S [M+Na]$^+$, 219.19, found: 219.

2.10. Synthesis of N-substituted (substituted 5-benzylidine)-thiazolidine-2,4-dione (3F-3R).

0.46 g (20 mM) Solid sodium hydride was slowly added to the stirred solution of 5-benzylidine thiazolidine-2,4-dione (1.0035 g, 4.5 mM in 30 mL of anhydrous DMF). The reaction mixture was stirred at ambient temperature until hydrogen gas bubbles had stopped.

The transparent solution with suspended sodium hydride particles thus obtained was filtered. The filtrate was added dropwise to a solution of alkyl halides (11.25 mM in 20 mL of anhydrous DMF). Resulting reaction mixture was stirred at ambient temperature under nitrogen atmosphere for 1 h.

The progress of the reaction was monitored by TLC (petroleum ether- ethylacetate 75:25, v/v). The solvent was removed using a vacuum rotary evaporator at 50ºC. The thick solution; left after evaporation of DMF; was washed with hexane several times to remove excess alkyl halides. Finally, it was dried under vacuum overnight in a vacuum desiccator over fused calcium chloride. The solid products obtained utilizing above cited procedures were denoted as (3F-3R).The schematic representation of the formation of (3F-3R)is given in Scheme 1.

2.11.3-butyl-5-[(chlorophenyl)methylidine]-thiazolidine-2,4-dione (3F).

Yield: 75.0%, mp 187-191ºC, Anal. Calcd: C (56.85%), H (4.77%), Cl (11.99%), N (4.74%), O (10.82%), S (10.84%), found C (56.84%), H (4.78%), Cl (11.98%), N (4.75%), O (10.83%), S (10.85%); I.R. (KBr pellets, cm^{-1}): 3500 (υC-H aromatics) 1750 (υC=O)sym, 1210 (υC-S-C); ^{1}H NMR (400 MHz, CDCl$_3$) δ(ppm): 7.87 (s, 1H, -CH=C), 7.52 (m, 2H, Ar-H), 7.21 (m, 2H, Ar-H), 3.80 (t, 2H, N-CH$_2$, J = 8.0Hz), 1.67 (m, 2H, -CH$_2$-), 1.38 (m, 2H, -CH$_2$-), 0.97 (t, 3H, -CH$_3$, J =4Hz). ESI-MS (m/z) Calcd for C$_{14}$H$_{14}$ClNO$_2$S [M+Na]$^+$, 295.78, found: 296.6.

2.12. 5-[(chlorophenyl)methylidine]-3-(propan-2-yl)-thiazolidine-2,4-dione (3G).

Yield: 70%, mp 175ºC, Anal. Calcd: C (55.42%), H (4.29%), Cl (12.58%), N (4.97%), O (11.36%), S (11.38%), found (55.43%), H (4.28%), Cl (12.54%), N (4.94%), O (11.33%), S (11.32); I.R. (KBr pellets, cm^{-1}): 2998.00 (υC-H aromatics), 1680 (υC=O)sym, 1500 (υCH=C), 1180 (υC-S-C); ^{1}H NMR (400 MHz, DMSO-d$_6$)δ (ppm): 7.85 (s, 1H, CH=C), 7.47 (m, 4H, Ar-H), 3.80 (m, 1H, (CH$_3$)$_2$CH-), 1.69(d, 6H, J= 8.0Hz, -(CH$_3$)$_2$-). ESI-MS (m/z) Calcd for C$_{13}$H$_{12}$ClNO$_2$S [M+Na]$^+$: 281.75, found: 281.20.

2.13.(5Z)-5-[(4-flurophenyl)methylidine]-3-propyl-1,3-thiazolidine-2,4-dione (3H).

Yield: 63%, mp 177-180 °C, Anal. Calcd: C (58.85%), H (4.56%), F (7.16%), N (5.28%), O (12.06%), S (12.09%), found C (58.77%), H (4.55%), F (7.14%), N (5.25%), O (12.04%), S (12.08%); I.R. (KBr pellets, cm^{-1}): 3100.00 (υC-H aromatics), 1610 (υC=O)sym, 1400 (υCH=C), 970 (υC-S-C); ^{1}H NMR (400 MHz, CDCl$_3$) δ(ppm): 7.88 (s, 1H, -CH=C), 7.55(m, 2H, Ar-H), 7.23(m, 2H, Ar-H), 3.80 (t, 2H, N-CH$_2$, J = 8.0Hz), 1.72 (m, 2H, -CH$_2$-), 1.00 (t, 3H, -CH$_3$, J =8 Hz); ^{13}C NMR (400 MHz, CDCl$_3$) δ (ppm): 166.30, 164.95, 163.21, 161.20, 130.93, 128.17, 119.86, 115.24, 40.51, 18.56, and 12.23; ESI-MS (m/z) Calcd for C$_{13}$H$_{12}$FNO$_2$S, 265.3 found [M+Na+4H]$^+$: 269.

2.14. 5-[(4-flurophenyl)methylidine]-3-(propan-2-yl)-thiazolidine-2,4-dione (3I).

Yield: 69%, mp 178-184°C, Anal. Calcd: C (58.85%), H (4.56%), F (7.16%), N (5.28%), O (12.06%), S (12.09%), found C (58.85%), H (4.56%), F (7.16%), N (5.28%), O (12.06%), S (12.09%); I.R. (KBr pellets, cm^{-1}): 2980.00 (υC-H aromatics), 1500 (υC=O)sym, 1450 (υCH=C), 980 (υC-S-C); ^{1}H NMR (400 MHz, CDCl$_3$) δ(ppm): 7.31 (s, 1H, -CH=), 6.90-7.28(m, 4H, Ar-H), 3.25-3.92 (m, 1H, N-CH-), 1.27 (m, 6H, - (CH$_3$)$_2$; ESI-MS (*m/z*) Calcd for C$_{13}$H$_{12}$FNO$_2$S [M+Na]$^+$: 265.3, found: 264.6;

2.15. 5-[(4-flurophenyl)methylidine]- 3-methyl-thiazolidine-2,4-dione (3J).

Yield: 60%, mp 163-164°C, Anal. Calcd: C (55.69%), H (3.4%), F (8.01%), N (5.9%), O (13.49%), S (13.52%), found C (55.68%), H (3.4%), F (8.04%), N (5.9%), O (13.49%), S (13.56%); I.R. (KBr pellets, cm^{-1}): 3042.43 (υC-H aromatics), 1731.57 (υC=O)sym, 1586.40 (υCH=C), 1225.96 (υC-S-C), 1355.66 (υ-N-); ^{1}H NMR (400 MHz, DMSO-d$_6$)δ (ppm): 7.95 (s, 1H, -CH=), 7.73(m, 2H, Ar-H), 7.42(m, 2H, Ar-H), 3.10 (s, 3H, N-CH$_3$); ESI-MS (*m/z*) Calcd for C$_{11}$H$_8$FNO$_2$S [M+Na]$^+$: 237.50, [M+Na+ 2H]$^+$, found: 239.

2.16. 3-benzyl-5-[(4-flurophenyl)methylidine]-thiazolidine-2,4-dione (3K).

Yield: 60%, mp 144-145°C, Anal. Calcd: C (65.16%), H (3.86%), F (6.06%), N (4.47%), O (10.21%), S (10.23%), found C (65.18%), H (3.82%), F (6.08%), N (4.45%), O (10.23%), S (10.21%). I.R. (KBr pellets, cm^{-1}): 3010 (υC-H aromatics), 1610 (υC=O)sym, 1250 (υC-S-C); ^{1}H NMR (400 MHz, DMSO-d$_6$)δ (ppm): 8.21 (m, 2H, Ar-H), 7.85 (s 1H,-CH=C), 7.91(m, 2H, Ar-H), 7.23(m, 5H, Ar-H), 4.10 (s, 2H, -CH$_2$-); ESI-MS (*m/z*) Calcd for C$_{17}$H$_{12}$FNO$_2$S: 313.3, [M+Na-3H]$^+$found: 310.6.

2.17.3-butyl-5-[(4-methoxyphenyl)methylidine]-thiazolidine-2,4-dione (3L).

Yield: 70%, mp 114-117°C, Anal. Calcd: C (61.83%), H (5.88%), N (4.81%), O (16.47%), S (11.01%), found C (61.77%), H (5.90%), N (4.84%), O (16.50%), S (11.22%); I.R. (KBr pellets, cm^{-1}): 3000 (υC-H aromatics), 1600 (υC=O), 1200 (υC-S-C); ^{1}H NMR (400 MHz, DMSO-d$_6$)δ (ppm): 7.89(s, 1H, CH=C), 7.61(m, 2H, Ar-H), 7.12(m, 2H, Ar-H), 3.83 (s, 3H, -OCH$_3$), 3.66 (t, 2H, J= 7.12Hz, -CH$_2$-N), 1.59-1.512(m, 2H, -CH$_2$-), 1.32-1.23(m, 2H, - CH$_2$-), 0.91(t, 3H, J= 7.32Hz, -CH$_3$); ESI-MS (*m/z*) Calcd for C$_{15}$H$_{17}$NO$_3$S [M+Na]$^+$:291.3, found: 291.

2.18.3-butyl-5-[(4-nitrophenyl)methylidine]-thiazolidine-2,4-dione (3M).

Yield: 73%, mp 139-140°C, Anal. Calcd: C (54.89%), H (4.61%), N (9.14%), O (20.89%), S (10.47%), found C (54.91%), H (4.70%), N (9.20%), O (20.90%), S (10.51%); I.R. (KBr pellets, cm^{-1}): 3010.00 (υC-H aromatics), 1720 (υC=O)sym, 1515 (υCH=C), 1350 (υC-S-C); ^{1}H NMR (400 MHz, DMSO-d$_6$)δ (ppm): 8.35(m, 2H, Ar-H), 8.03 (s, 1H, -CH=), 7.89(d, 2H, Ar-H) 3.6773(t, 2H, J= 7.08Hz, -CH$_2$-N), 1.60-1.53(m, 2H, -CH$_2$-), 1.33-1.24(m, 2H, - CH$_2$-), 0.9115(t, 3H, J= 7.24Hz,CH$_3$); ^{13}C NMR (400 MHz, CDCl$_3$) δ (ppm): 166.80 (-C=O from N-amide) 165.80 (-C=O from N-amide), 147.99 (Ar-C attached to nitro group) 139.37 (ethylene CH=C), 130.32(Ar-C), 126.27 (Ar-C), 124.40 (Ar-C), 123.37(-ethylene C), 42.24 (CH$_2$), 29.76 (CH$_2$), 19.97 (CH$_2$), 13.63(CH$_3$); ESI-MS (*m/z*) Calcd for C$_{14}$H$_{14}$N$_2$O$_4$S [M+Na]$^+$: 306.338, found: 305.8.

2.19. 5-[(4-nitrophenyl)methylidine]-3-(propan2-yl)-thiazolidine-2,4-dione (3N).

Yield: 65%, mp 192.5 °C; Anal. Calcd: C (53.52%), H (4.21%), N (9.60%), O (21.90%), S (10.95%), found C (53.42%), H (4.14%), N (9.58%), O (21.89%), S (10.97%); I.R. (KBr pellets, cm^{-1}): 3015.00 (υC-H aromatics), 1715 (υC=O)sym, 1525 (υCH=C), 1350 (υC-S-C); ^{1}H NMR (400 MHz, DMSO-d$_6$)δ (ppm): 8.35(m, 2H, Ar-H), 7.99 (s, 1H, CH=C), 7.86(m, 2H, Ar-H) 4.57-4.51(m, 1H, (CH$_3$)$_2$CH-), 1.41(d, 6H, J=

6.88Hz, -(CH$_3$)$_2$-); ESI-MS (*m/z*) Calcd for C$_{13}$H$_{12}$N$_2$O$_4$S [M+Na]$^+$: 292.3: found 291.8.

2.20. 3-methyl-5-[(4-nitrophenyl)methylidine]-thiazolidine-2,4-dione (3O).

Yield: 64%, mp 225-230°C, Anal. Calcd C (50%), H (3.05%), N (10.6%), O (24.22%), S (12.13%), found C (50%), H (3.10%), N (10.55%), O (24.30%), S (12.21%); I.R. (KBr pellets, cm^{-1}): 3009.00 (υC-H aromatics), 1700 (υC=O)sym, 1515 (υCH=C), 1340 (υC-S-C); ^{1}H NMR (400 MHz, DMSO-d$_6$)δ (ppm): 8.37(m, 2H, Ar-H), 8.05 (s, 1H, -CH=C), 7.91(d, 2H, Ar-H), 3.13(s, 3H, N-CH$_3$). ESI-MS (*m/z*) Calcd for C$_{11}$H$_8$N$_2$O$_4$S [M+Na]$^+$: 264.2: found 263.

2.21.3-benzyl-5-[(4-nitrophenyl)methylidine]-thiazolidine-2,4-dione (3P).

Yield: 60%, mp 193-195°C, Anal. Calcd: C (59.99%), H (3.55%), N (8.23%), O (18.8%), S (9.42%), found C (59.85%), H (3.65%), N (8.15%), O (18.7%), S (9.33%); I.R. (KBr pellets, cm^{-1}): 3050.00 (υC-H aromatics), 1710 (υC=O)sym, 1515 (υCH=C), 1350.40 (υC-S-C); ^{1}H NMR (400 MHz, DMSO-d$_6$)δ (ppm): 8.37 (m, 2H, Ar-H), 8.09(s, 1H,-CH=C), 7.91(m, 2H, Ar-H), 7.38(m, 5H, Ar-H), 4.86 (s, 2H, -CH$_2$-); ESI-MS (*m/z*) Calcd for C$_{17}$H$_{12}$N$_2$O$_4$S [M+Na]$^+$: 340.3, found: 339.

2.22.3-butyl-5-[(4-methylphenyl)methylidine]-thiazolidine-2,4-dione (3Q).

Yield: 70%, mp 188-189 °C, Anal. Calcd: C (65.43%), H (6.22%), N (5.09%), O (11.62%), S (11.64%) found C (65.50%), H (6.32%), N (5.14%), O (11.72%), S (11.54%); I.R. (KBr pellets, cm^{-1}): 3020.00 (υC-H aromatics), 1610 (υC=O)sym, 1515 (υCH=C), 1250 (C-S-C); ^{1}H NMR (400 MHz, DMSO-d$_6$)δ (ppm): 7.89 (s, 1H, CH=C), 7.62 (m, 2H, Ar-H), 7.13 (m, 2H, Ar-H), 3.83(s, 3H, Ar-CH$_3$), 3.66(t, 2H, J= 7.08Hz, -CH$_2$-N), 1.59-1.51 (m, 2H, -CH$_2$-), 1.32-1.22(m, 2H, - CH$_2$-), 0.90 (d, 3H, J= 7.28Hz, -CH$_3$); ESI-MS (*m/z*) Calcd for C$_{15}$H$_{17}$NO$_2$S [M+Na]$^+$: 275.36, found: 275.20.

2.23. 5-[(4-methylphenyl)methylidine]-3-propan-2yl)-thiazolidine-2,4-dione (3R).

Yield: 65%, mp 166-170 °C, Anal. Calcd: C (64.34%), H (5.79%), N (5.36%), O (12.24%), S (12.27%), found C (64.44%), H (5.79%), N (5.46%), O (12.36%), S (12.27%); I.R. (KBr pellets, cm^{-1}): 3010.00 (υC-H aromatics), 1600 (υC=O)sym, 1515 (υCH=C), 1250 (υC-S-C); ^{1}H NMR (400 MHz, DMSO-d$_6$)δ (ppm): 7.85 (s, 1H, CH=C), 7.52(m, 2H, Ar-H), 7.367 (m, 2H, Ar-H), 4.57-4.50(m, 1H, (CH$_3$)$_2$CH-), 2.3620(s, 3H, Ar-CH$_3$), 1.39 (d, 6H, J=6.92 -(CH$_3$)$_2$; ESI-MS (*m/z*) Calcd for C$_{14}$H$_{15}$NO$_2$S [M+Na]$^+$: 261.33, found: 260.70.

2.24. X-ray crystal structure determination.

Slow evaporation of methane solutions of **3H** compound gave very good quality single crystal. The crystal was mounted on a capillary. X-ray diffraction studies of the crystal were carried out on a BRUKER AXS SMARTAPEX diffractometer with a CCD area detector (KR) 0.710 73 Å, with graphite monochromator SMART B 2000 [20]. Frames were collected at T = 293 K by ω, φ, and 2θ-rotation at 10 s per frame with SAINT [21].

The measured intensities were reduced to F2 and corrected for absorption with SADABS.28 Structure solution, refinement, and data output were carried out with the SHELXTL program [22]. Non-hydrogen atoms were refined anisotropically. C−H hydrogen atoms were placed in geometrically calculated positions by using a riding model. Images were created with the Mercury program [23]. CCDC 1468802 contains the supplementary crystallographic data for the structure reported in this paper. These data can be obtained free of charge via http://www.ccdc.cam.ac.uk/conts/retrieving.html, or from the Cambridge Crystallographic Data Centre, 12 Union Road, Cambridge CB2 1EZ, UK. Fax: (+44) 1223 336 033; or e-mail: deposit@ccdc.cam.ac.uk.

2.25. Anticancer Assays.

The *in vitro* anticancer profiles of the synthesized compounds were determined against a human liver cancer cell line; Hep-G2, by a cell cytotoxicity assay (LDH assay). Hep-G2 cells were cultured in a medium containing 87% Minimum Essential Medium (MEM), 2.2 g/L sodium bicarbonate, 10% fetal bovine serum, 1% sodium pyruvate, 1% non-essential acid, and 1% antibiotic-antimycotics. 5000 Cells per well were seeded on a 96-well plate for 3days. At a confluence of 99.7%, 201 mg/mL stock solutions of tested drugs were prepared in dimethyl sulfoxide. The cells were exposed to 10, 1, 0.1, and 0.01 µg/mL concentrations of the compounds diluted by culture medium after seeding for 24 h.

2.26. DNA Binding.

UV–vis absorption spectrophotometry was used to study the interactions of derivatives of thiazolidine-2,4-dione and their *N*-Substituted analogues with Ct-DNA at 7.4 pH in double distilled water containing tris-(hydroxymethyl)-amino methane (Tris, 10^{-2} M) [24, 25]. The concentration of the freshly prepared Ct-DNA solution was determined spectrophotometrically at 260 nm ($\varepsilon = 6600\text{M}^{-1}$ cm^{-1}) [26].The binding experiments were carried out by recording the absorbance changes on adding increasing concentrations of DNA (0.3×10^{-5}–1.7×10^{-5} M) against a fixed concentrations of thiazolidine-2,4-dione derivatives and their *N*-Substituted analogues (0.2×10^{-7} M).

Firstly, the values of λ_{max} and absorbance of pure DNA and different compounds in buffer solutions were recorded. After that the values of λ_{max} and absorbance were recorded every time by adding 2.0 mL of DNA solution to fixed concentration of the different compounds. The absorption spectra were recorded after each addition of the various concentrations of DNA solution (2.0 mL). Benssi-Hilderbrand equation modified by Wolfe *et al.,* was used for the determination of intrinsic binding constant (K_b) [27].The equation is as follows:

$$\frac{[DNA]}{(\varepsilon_a - \varepsilon_f)} = \frac{[DNA]}{(\varepsilon_a - \varepsilon_f)} + \frac{1}{K(\varepsilon_b - \varepsilon_f)}$$

where, absorption coefficients ε_a, ε_f, and ε_b correspond to A_{obs} / [compounds], extinction coefficients for the compounds and the extinction coefficient for the compounds in the fully bound form, respectively. The binding constants for the different compounds (K_b) were determined by the slopes and the intercepts of the plots of $\frac{[DNA]}{(\varepsilon_a - \varepsilon_f)} vs [DNA]$.

2.27. *In silico* studies.

Docking studies of the compounds were performed by Intel® dual CPU (1.86 GHz) with Windows XP operating system. Marwin sketch software was used for drawing 3D structures of the compounds. The 3D structures so obtained were converted to the pdb file format. The preparation of the compounds were carried out by assigning Gastegier charges, merging non-polar hydrogens, and saving in PDBQT file format using AutoDock Tools (ADT) 4.2 [28]. X-ray crystal structure of DNA (PDB ID: 1BNA) wasobtained from the Protein Data Bank [29]. By using AutoDock Tools (ADT) 4.2 hetero-atoms (water molecules) were removed from DNA and saved in PDB file format. Gastegier charges were assigned to DNA and saved in PDBQT file format using ADT.

The preparation of parameter files for grid and docking was done using ADT software. Docking was performed with AutoDock 4.2 (Scripps Research Institute, USA), considering all the rotatable bonds of ligand as rotatable and receptor as rigid [30]. The grid box size of 60 × 80 × 110 Å with 0.375 Å spacing was used that included whole DNA. In the present work, a plugin for PyMOL was described, which allowed to carry out the molecular docking, virtual screening, and binding site analysis with PyMOL. The plugin represented an interface between PyMOL and two popular docking programs i.e. AutoDock (4.2) [31,32] and AutoDock Vina[33].The combined effect of these two software made extensive use of a Python script collection (AutoDock Tools) for the setup of docking runs [28].

2.28. Solution stability.

A qualitative insight into the stability of the compounds at physiological pH was obtained by monitoring their UV-vis spectra in 5% DMSO solutions of PBS at pH 7.4, over a period of 36 h. The solutions of the compounds (10^{-4} M) were prepared in 5% DMSO solutions of PBS at pH 7.4. The hydrolysis profiles of the compounds were assessed by recording their electronic spectra over 36 h time period at 25 ºC.

3. RESULTS SECTION

3.1. Chemistry.

Thiazolidine-2,4-dione moiety (2A) was prepared by using thiourea (1) and chloroacetic acid (2). The so-formed heterocyclic moiety was used to prepare derivatives of thiazolidine-2,4-dione (3A-3E; Knoevenagel's condensates) with *meta and para* substituted benzaldehyde *via* Knoevenagel's condensation. The final products [(3F-3R); Scheme 1] were prepared by substitution reactions of Knoevenagel's condensates (3A-3E) with alkyl bromide. All the compounds were washed with petroleum ether and hexane. By recording melting points, UV-Vis spectra and elemental analyses, the purities of all the compounds were confirmed. Spectroscopic techniques like FT-IR, ^{1}H NMR and ESI-MS were used for the determination of structures of the synthesized compounds. 3H compound was further characterized by X-ray analysis.

The formation of 3A-3E was confirmed by the presence of characteristic ^{1}H NMR peak of alkenic protons in the range of 7.41-8.05 ppm, whereas aromatic protons appeared in the range of 7.12-8.37 ppm. The solid state FT-IR spectra of 3A-3E showed characteristic bands at 2900-3100 cm^{-1} (C-H aromatics), 1500-1720 cm^{-1} (C=O), 1400-1550 cm^{-1} (CH=C) and 800-1310 cm^{-1} (C-S-C). The peculiar ESI-MS (*m/z*) peaks were found at, 239 for 3A, 223 for 3B, 235 for 3C, 250 for 3D and 219 for 3E; confirming the formation of Knoevenagel's condensates. The final *N*-substituted derivatives (3F-3R) were characterized by ^{1}H NMR and ESI-MS .In ^{1}H NMR alkyl protons appeared in the range of 0.91-3.66 ppm in addition to aromatic and alkenenic protons. Moreover, the mass spectra of 3F, 3G, 3H, 3I, 3J, 3K, 3L, 3M, 3N, 3O, 3P, 3Q and 3R showed peaks at *m/z* values of 296.6, 281.20, 269, 264.6, 239, 310.6, 291, 305.8, 291.8, 263.6, 339, 275.20 and 260.70, respectively. These spectral studies confirmed that the compounds were formed as per Scheme 1. The reported compounds, used in the cytotoxic studies were stable to air and had good stabilities in 5% DMSO solutions of PBS at physiological pH.

3.2. Single crystal structure of 3H.

Out of the synthesized compounds 3H compound [(5Z)-5-[(4-flurophenyl)methylidine]-3-propyl-1,3-thiazolidine-2,4-dione] crystallized from methane solution as a colorless prism (Figure1).
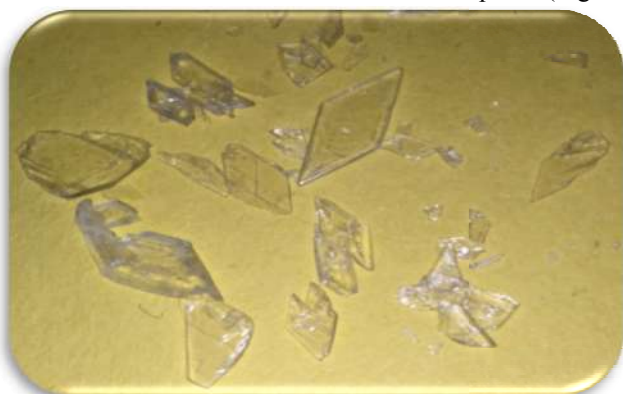

Figure 1. Colorless crystals of3H.

ORTEP representation of 3H has been shown in Figure 2.Hydrogen bonds were not found in the structure. The crystal structure of 3H shows two types of rings- benzene unit (1) and thiazolidine unit (2) (Figure 3). The benzene ring at C4 is attached to C8 of (2) through methine bridging. The ring (2) is attached to propyl group through N1. In addition to it ring (2) contains two oxygen atoms (O1, O2) attached to C9 and C10 respectively. The ring (1) is bonded to fluorine (F1) atom at C1.
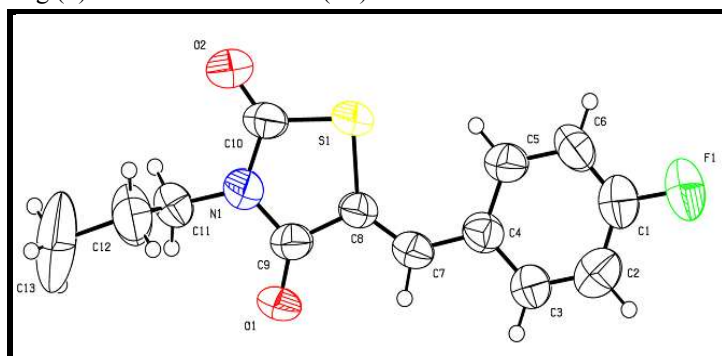

Figure 2. ORTEP plot for the compound 3H. All the non-hydrogen atoms are presented by their 30% probability ellipsoids.

The O2, O1 of ring 2 with H5 of ring (2) and H7 of methine carbon (C7) respectively shows the H-bonding interaction in the crystal packing. In addition to it weak Van der waals forces exist between sulphur atoms (S1 and S1) of two molecules. A special type of interaction exists between H11A and π-electron cloud of methine carbon. It is clear from the Figure 3 that a molecule possesses Cs symmetry.
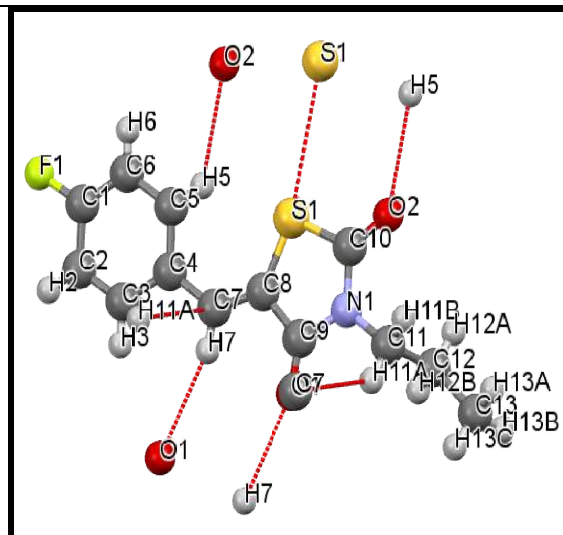

Figure 3. Crystal packing of 3H. Hydrogen bondings are presented in dashed red lines.

The benzene and bulky group in the thiazolidine ring possess a little distortion in the planarity. This planarity loss is related to the crystal packing forces increasing the stress of its structure. Crystal data and details of the data collection and refinement for the compound 3H are mentioned in Table 2. Table 3 contains selected bond lengths and angles for compound 3H.

Table 2. Crystal data and structure refinement for 3H.

Compound	3H
Formula	$C_{13}H_{12}FNO_2S$
Formula weight	265.30
T (K)	296 K
Wavelength (Å)	0.71073
Crystal System	Triclinic
Volume	691.23 (16)
Space group	P-1
Hall group	-P 1
Bond precision C-C (Å)	0.0117
a (Å)	5.2435(8)
b (Å)	9.7709(12)
c (Å)	14.3281(19)
α (°)	74.787(7)
β (°)	80.905(8)
γ(°)	79.215(7)
V (Å^3)	691.23(16)
Z (Å)	2
F_{000}	276.0
D_{calc} (g cm^{-3})	1.275
μ (mm^{-1})	0.229
h, k, l max	5,10,14

Table 3. Bond lengths (Å) and angles (°) for **3H**.

Bond lengths (Å)		Bond angles (°)		Bond angles (°)	
C(1)-C(2)	1.41(1)	C(2)-C(1)-C(6)	121.9(9)	C(9)-C(8)-S(1)	110.9(5)
C(1)-C(6)	1.34(1)	C(2)-C(1)-F(1)	117.2(8)	C(8)-C(9)-N(1)	110.2(6)
C(1)-F(1)	1.345(9)	C(6)-C(1)-F(1)	120.9(8)	C(8)-C(9)-O(1)	126.6(7)
C(2)-C(3)	1.36(1)	C(1)-C(2)-C(3)	118.4(9)	N(1)-C(9)-O(1)	123.2(7)
C(3)-C(4)	1.40(1)	C(2)-C(3)-C(4)	122.0(8)	N(1)-C(10)-O(2)	124.3(7)
C(4)-C(5)	1.400(9)	C(3)-C(4)-C(5)	117.4(7)	N(1)-C(10)-S(1)	111.0(5)

Bond lengths (Å)		Bond angles (º)		Bond angles (º)	
C(4)-C(7)	1.446(9)	C(3)-C(4)-C(7)	119.8(7)	O(2)-C(10)-S(1)	124.7(6)
C(5)-C(6)	1.39(1)	C(5)-C(4)-C(7)	122.8(6)	C(12)-C(11)-N(1)	112.7(6)
C(7)-C(8)	1.336(9)	C(4)-C(5)-C(6)	121.1(7)	C(11)-C(12)-C(13)	110.1(8)
C(8)-C(9)	1.472(9)	C(1)-C(6)-C(5)	119.2(8)	C(9)-N(1)-C(10)	116.3(6)
C(8)-S(1)	1.742(6)	C(4)-C(7)-C(8)	132.3(7)	C(9)-N(1)-C(11)	121.7(6)
C(9)-N(1)	1.391(9)	C(7)-C(8)-C(9)	121.2(6)	C(10)-N(1)-C(11)	121.9(6)
C(9)-O(1)	1.201(8)	C(7)-C(8)-S(1)	127.9(6)	C(8)-S(1)-C(10)	91.7(3)
C(10)-N(1)	1.377(9)				
C(10)-O(2)	1.218(9)				
C(10)-S(1)	1.760(7)				
C(11)-C(12)	1.51(1)				
C(11)-N(1)	1.464(8)				
C(12)-C(13)	1.65(1)				

3.3. Cytotoxic Profiles.

The cytotoxic activities of the reported compounds (2A-3R) were evaluated on HepG2 cells. The IC_{50} values determined are given in Table 4. The cytotoxic activities of the compounds are shown in Figure 4. It was observed that at 10 μg/mL concentration, 2A, 3A, 3F, 3G, 3B, 3I, 3K, 3L and 3E-IV showed apparentcytotoxicities. However, 3Fwas not active against HepG2 cells at this concentration while as, 3C, 3Q and 3R showed mild toxicities.Besides, it was observed that 3D 3H, 3J and 3Q had high toxicities in 48 h. At 1.0 μg/mL 2A, 3A, 3B, 3F and 3G showed apparent toxicities while as, 3D, 3H, 3I, 3Q and 3R were non-toxic. At 0.1 μg/mL 2A, 3A, 3B, 3C, 3F, 3G, and 3L showed moderate toxicities. At 0.01 μg/mL 2A, 3A, 3B, 3C, 3F, 3G, and 3I showed good cytotoxicities, while the othercompounds were non-toxic.

Finally, it was observed that the compounds 2A, 3A, 3B, 3F, 3G, 3H, 3K & 3Q at 10 μg/mL concentrations were the most toxic to HepG2 cells; considered as active compounds (Figure 4).
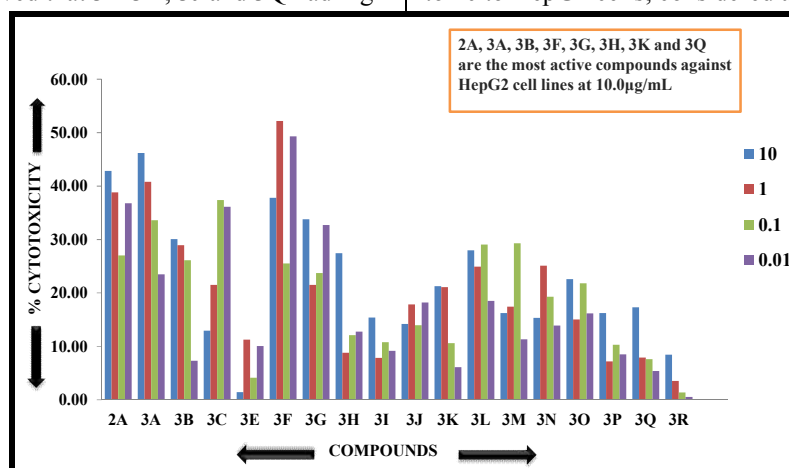

Figure 4. Percentage cytotoxicitiesof **2A-3R** against HepG2 cell line within the concentration range of 0.01-10.0 μg/mL.

Table 4. IC_{50} values of **2A-3R** after 72 h incubation with HepG2 cells.

Compounds	IC_{50} (μM)	Compounds	IC_{50} (μM)
2A	17.19	3J	137.95
3A	12.03	3K	37.77
3B	27.75	3L	63.99
3C	-8.37	3M	90.91
3D	314.38	3N	86.96
3E	-59.87	3O	289.63
3F	22.38	3P	234.75
3G	32.71	3Q	40.24
3H	24.03	3R	68.53
3I	66.68		

3.4. DNA Binding.

DNA is one of the most important pharmacological targets of anticancer drugs [24, 25, 34]. Therefore, it is worthwhile to study the interactions of the compounds with DNA to have a clue into their anticanceractivities and possible mechanisms of action.

Generally, covalent and non-covalent binding takes place between a compound and DNA. In covalent binding, a labile compound is replaced with a nitrogen atom of DNA base, such as N^7 of guanine. In case of non-covalent binding, the interactions like intercalative, electrostatic and groove binding are possible [4]. Usually, changes in absorbance or wavelength or both are indicative of the interactions and intercalative modes involving strong stacking interactions among aromatic chromophores and the base pairs of DNA [35]. Itis supposed that hyperchromism involves covalent binding and bathochromism is due to breakage of the secondary structure of DNA. Additionally, the existence of the red shifts indicates coordination of the compounds with DNA through the N^7 position of guanine [36]. Furthermore, outside groove binding is characterized by no or minor change in UV-Vis. spectra; generally with minor hyperchromicity [37].

The electronic absorption bands of thiazolidine-2,4-dione derivatives (3A - 3R) in the absence and presence of DNA are shown in Figure. FS1 a–n (Supplementary data). The absorption spectra of the compounds exhibited peaks in the range of 200–400 nm. The small shifts of the bands were observed in the region of 300–400 nm by the addition of DNA due to intra ligand $\pi\rightarrow\pi^*$ and $n\rightarrow\pi^*$ transitions [38,39]. These small shiftings of the bands indicated bathochromic shifts of all the compounds due to the interactions with DNA. Moreover, with the addition of different concentrations $(0.3\times10^{-5}–1.7\times10^{-5}M)$ of DNA, hypo-chromaticities were observed for all the compounds. Thus, these changes indicated the formation of DNA adducts [40]. It is interesting to note that covalent and non-covalent bonding might be responsible for these hypochromic shifts, which had been observed in all the compounds [41]. UV-vis data for compounds [3A- 3R) are given in Table 5 and Table TS1 (Supplementary data).

For a ready reference, the absorption spectra of three compounds (3A, 3F, and 3M; $0.2 \times 10^{-7}M$); both in the absence and presence $(0.3\times10^{-5}–1.7\times10^{-5}M)$ of Ct-DNA are given in Figure 5. Furthermore, the values of DNA binding constants of all the compounds ranged from 7.07×10^2-2.50×10^8 M^{-1}, indicating good interactions with DNA. The regression analysis was carried out using Microsoft Excel program for DNA binding studies. It was found that the correlation coefficients (R^2) ranged from 0.7512-1.000%. The order of DNA binding constants of the synthesized compounds was 3A >3F > 3B > 3H >3G>3K>3Q >3D > 3L> 3C >3I >3E>3N>3P > 3J >3R>3M>3O. Finally, it can be concluded that nearly all the compounds intercalated through the minor groove with Ct-DNA which is well supported by the available literature [42].

The literature clearly indicates that the compounds forming adducts with DNA through minor grooves, and the adducts were mainly stabilized by hydrogen bonds and hydro-phobic interactions [43, 44]. All these facts are well supported by the simulation studies. DNA titration experiments can be seen in Figure 5 and Figure FS1 a-n.
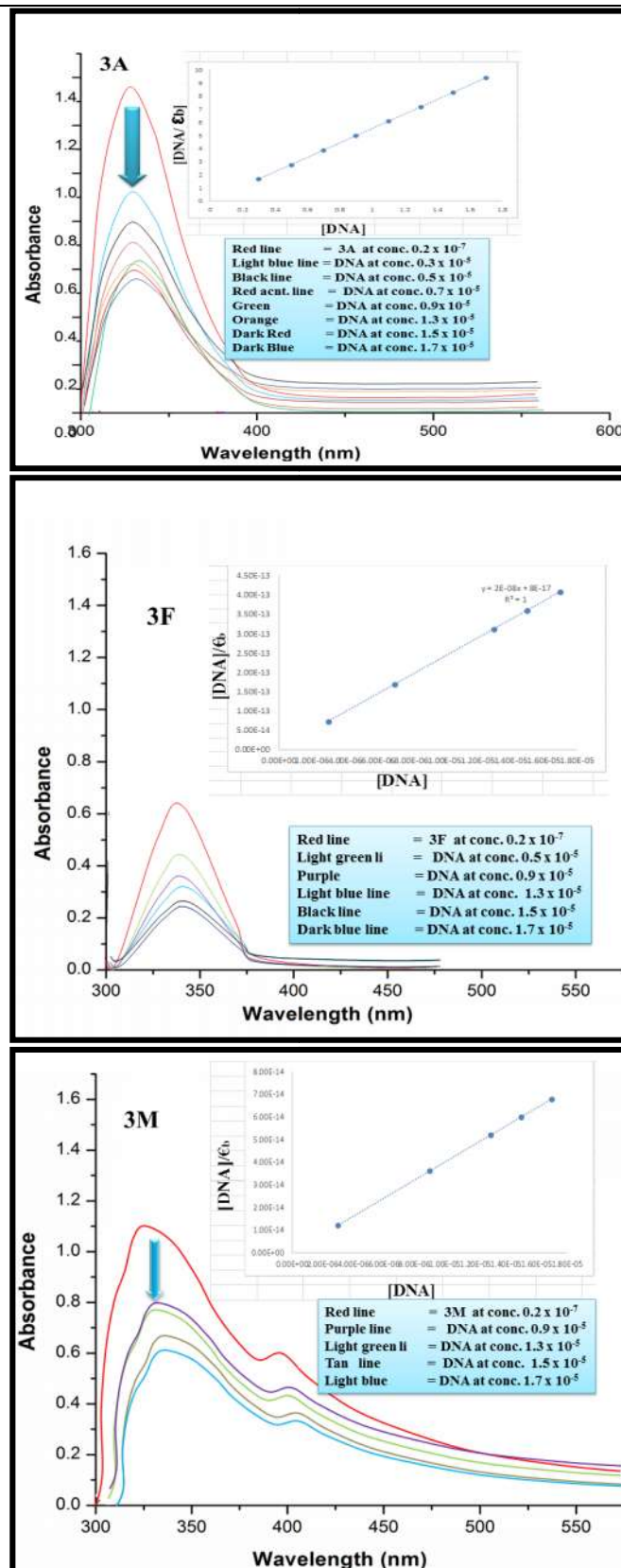

Figure 5. Absorption spectra of 3A, 3F and 3M (0.2×10^{-7} M) in the absence (red line) and presence (other coloured lines) of increasing DNA concentrations; 0.3×10^{-5}M -1.7 $\times10^{-5}$M respectively. Arrow indicates the hypochromic shifts on increasing DNA concentrations. Inset: plots of [DNA]/ϵ_b (M^2cm^{-1}) versus [DNA] for the titration of Ct-DNA with compounds.

Additionally, it is interesting to mention here that the compounds containing halogen atoms (3A,3B,3F,3G,3H and 3Q) had high affinity for DNA (higher K_b values) than the compounds containing halogen groups (chloro and fluoro). Furthermore, the

compounds containing methoxy group had better DNA binding affinities than the compounds having nitro groups. Overall, the differently substituted compounds showed binding in the order as, halogen >methyl > methoxy > nitro, groups.

3.5. In Silico Studies.

Molecular docking is a useful tool for predicting the interactions of anticancer agents with various macromolecules at the supramolecular level. This section describes docking interactions of the developed molecules with DNA. Most common form of DNA is B-DNA, which has characteristic wide and major deep grooves and narrow and deep minor grooves. The specificity of base pairing between two DNA strands gives distinct hydrogen bond acceptor/donor patterns in major and minor grooves. To find out the possible sites of DNA interactions with the reported compounds, the molecular DNA docking of the compounds had been carried out using AutoDock (4.2) Vina tool.
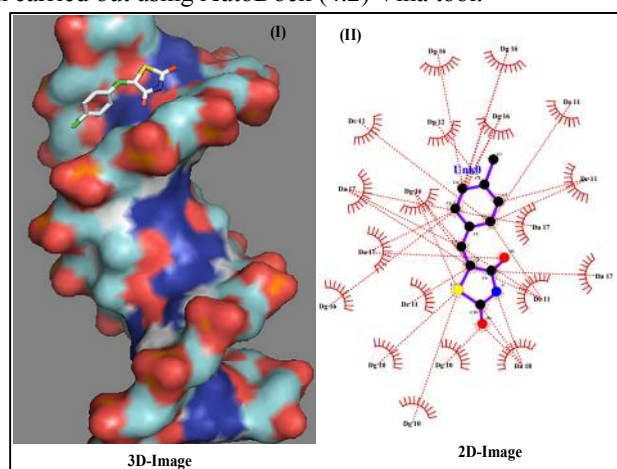

Figure 6a. 3D- and 2D-docking images of **3A** with DNA. Image (I) indicate the interaction of **3A** with DNA *via* minor groove, and image (II) indicates the interaction is mainly through hydrophobic attractions.

Figure 6b. 3D- and 2D- docking images of **3G** with DNA. Image (I) indicate the interaction of **3G** with DNA *via* minor groove, and image (II) indicates the interaction is mainly through hydrophobic attractions.

Figure 6c. 3D- and 2D- docking images of **3K** with DNA. Image (I) indicate the interaction of **3K** with DNA *via* minor groove, and image (II) indicates the interaction is mainly through hydrophobic attractions.
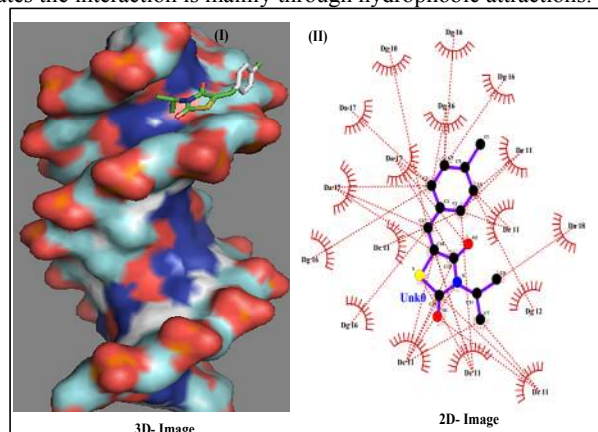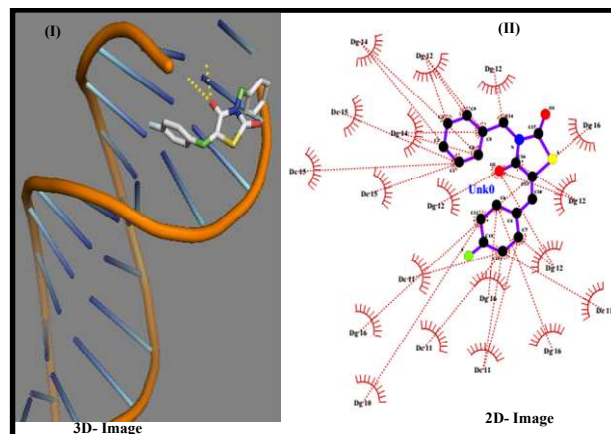
The docking studies of the compounds were performed with DNA dodecamers d(CGCGAATTCGCG)2 (PDB ID: 1BNA). The order of binding energies of the synthesized compounds was 3A >3B > 3F> 3G> 3H> 3K> 3Q= 3L> 3C= 3D= 3N= 3O>3E= 3J> 3R> 3I. The docked models of 3A, 3G and 3K are shown in Figure 6a-c.

The docking models of the other reported compounds are shown in Figure FS2 a-o (supplementary data). It is clear from the docked models that all the compounds preferred DNA minor grooves. The number of H-bonds formed by the compounds 3A–3R is given in Table 6. There were no hydrogen bonds formed in 3A, 3D, 3F, 3G, 3I, 3J and 3R. One hydrogen bond with DNA was formed by 3B and 3H, two were formed by 3K, 3M and 3N, three hydrogen bonds by 3E, 3L, 3P and 3Q, and 3C and 3O formed four hydrogen bonds with DNA. It is interesting to note that a greater number of hydrogen interactions were observed in 3E series due to the presence of two oxygen atoms (nitro group). The order of binding energy among nitro compounds was 3P >3M >3D>3N, 3O. Also, it was observed that the ketonic and nitro moieties were the common groups involved in H-bonding. For example, in case of 3M two hydrogen bonds were observed (residues involved A: DC`23/O2:UNK0: O of the nitro group, B: DC`21/O2: UNK0: O of keto group). The different simulation parameters of the synthesized compounds are given in Table 6. During the process of DNA interactions, it had been observed that all the reported compounds oriented themselves in such a fashion that their benzene and thiazolidine rings were inside minor grooves.

Overall, the experimental results of DNA binding were in good agreement with those of docking studies. The compounds containing nitro substituents (e.g. 3P, binding affinity -6.6 kcal/mol) have more affinity than the compounds containing fluoro and chloro substituents (3K; binding affinity -6.6 kcal/mol, 3F, binding affinity -5.8 kcal/mol). Similarly, the compounds containing methoxy groups (3L, binding affinity -6.1 kcal/mol) had more affinity than compounds with methyl groups (3R, binding affinity -5.7 kcal/mol).

Table 5. Wavelength and hypochromic shifts, and binding constants of **3A-3R** on adding increasing concentrations of DNA (0.3×10^{-5}M -1.7×10^{-5}M). For details of wavelength and absorbance shifts, please see supplementary data.

Compounds	$\Delta\lambda_{max}$ (nm)	Hypochromism	K_b (M^{-1})
3A	1	0.646	2.50×10^8
3B	2	0.935	1.0×10^8
3C	1	0.631	5.0×10^6
3D	4	0.247	3.0×10^7
3E	1	0.376	2.0×10^6
3F	2	0.151	1.67×10^8
3G	2	0.018	7.50×10^7
3H	10	0.275	1.0×10^8
3I	1	0.06	2.0×10^6
3J	1`	0.532	2.0×10^5
3K	4	1.364	3.75×10^7
3L	2	0.350	5.0×10^7
3M	2	0.881	1.0×10^5
3N	12	0.628	1.25×10^6
3O	1	0.353	7.07×10^2
3P	2	0.834	4.4×10^5
3Q	1	0.453	3.70×10^7
3R	14	0.100	2.0×10^5

Table 6. Results of the molecular docking of **3A-3R** with DNA. Binding affinity, number of hydrogen bonds formed, residues involved in hydrogen bonding and hydrophobic interactions with DNA have been summarized.

Compounds	Binding affinity (kcal/mol)	Number of H-bonds with DNA	Residues involved in H-bonding	Residues involved in Hydrophobic interactions
3A	-6.6	0	-	**Dg10::** S **Dc11::** C1,C5,C6,C8,&C9 **Dg12::**C2 **Dg16::** C3,C4,C6,C8&S **Da17::** C3,C6,C8,C9&O2 **Da18::** O1,C10,N
3B	-6.3	1	DG`16/O3::UNK0:O of keto group	**Dg10::**C2 **Dc11::**C1,C2,C3,C4,C6,C8 and S **Dg12,Dg14::** S **Dg16::** C2,C6,C8,C9, N and O2 **Dg17::** C5,C6,C8 and O2
3C	-5.8	4	**A**:DG`16/O4:UNK0:N of amide linkage **B**:DG`16/O4::UNK0:O of keto group **C**:DG`16/N3::UNK0:O of keto group **D**:DC`15/O2::UNK0:O of keto group	**Dg10&Dc15::**C5 & N respectively. **Dc11::** C1,C2,C3,C4,C5 &S **Dg12::** S&O1 **Dg14::** C11 &S **Dg16::** C5,C9,C10&O2 **Da17::** C3,C6,C8,C9 &O3 **Da18::** C9&O3
3D	-5.8	0	-	**Dg10::** C5& C3 **Dc11::**C1C3,C4C5&C6 **Dg12::** C4&S **Dg16::** C8,C9,O2,O4&N **Da17::** O3&O4

Compounds	Binding affinity (kcal/mol)	Number of H-bonds with DNA	Residues involved in H-bonding	Residues involved in Hydrophobic interactions
				Da17::C5,C6,C8,O2&O4
3E	-5.5	3	**A**: DG`16/N2:: UNK0:O of keto group **B**:DC`11/O4::UNK0:O of keto group **C**:DG`10/N3::UNK0:O of keto group	**Dg10::** N of thiazolidine **DC11::**C1,C5,C7 of benzene and O2,C9,N of thiazolidine ring **Dg12::** C1,C5 of benzene **Dg14, Dc15::**C8 of methyl group. **Dg16::** C4 of benzene **Da17::** S of thiazolidine ring **Da18::** O1, C4 of thiazolidine ring
3F	-6.5	2	**A**: DG`4/N2:: UNK0:O of keto group **B**:DG`22/N2::UNK0:O of keto group -	**Da6::** C1,C4,C7,C10, O1 & S **Dg4,Dc21**:: C2,C3 C5 &C10 **Dg22::**C3,C5 **Dt7, Dt20::** O1& S
3G	-6.2	0	-	**Dg10,Dg12&Da18::**C4,C6 &C8 respectively. **Dc11::**C1,C4,C6,C10,C12,C13&O1 **Dg16::** C3,C4&C5 **Dg17::**C2,C3&C12
3H	-6.4	0	-	**Dg4::** C2&C6 **Da5::**S&C6 **Da6::** C4,C6,C10&S **Dt7::**C14&O1 **Dt20::** S **Dc21**:: C3, C7,C14,O1&S **Dg22::** C5
3I	-5.4	1	DG`22/N2::UNK0:O of keto group	**Dg2::** C6 **Dc3::**C6 **Dg4::**C2&C8 **Da5::** C4& S **Dg22::** C10 **Dg23::** C5 &C10 **Dg24::** C5
3J	-5.5	0	-	**Dc3::** C2 **Dg4::** C6, C7,C10&N **Da5::** C8&O2 **Dg22::** C1,C2,C4,C7 &S **Dg23::** C4&S
3K	-6.1	2	**A**:DC`11/O2::UNK0:O of keto group **B**:DG`12/O4:: UNK0:O of keto group	**Dg10&Dc15::**C12 &C1 respectively. **Dc11::** C7&C11 **Dg12::** C3,C5, C7,C9, C14,C16&O2 **Dg14::** C2,C5&C8 **Dg16::** C6,C12& S
3L	-5.9	3	**A**:DC`11/O4'::UNK0:O of keto group **B**:DG`16/N2::UNK0:O of keto group **C**: DG`10/N2:: UNK0:O of keto group	**Dc9::** C4&C13 **Dg10::**C2,C3,C4,C6,C8,C13&O3 **Dc11::**C10,C14&O2 **Dc15&Dt19::**C3&C13 resp. **Dg16::**C1,C3,C6&O2 **Da17::**C4,C5,O1&S **Da18::**C4,C7,C8,C11,C13&O3
3M	-5.6	2	**A**:DC`23/O2:: UNK0:O of nitro **B**: DC`21/O2:: UNK0:O of keto group	**Dg4&Da5::**C4&C8 **Da6::**C1,C3&C9 **Dt7,Dg22&Dc23::**C1,C8&C7 **Dt20::**C1 **Dc21::**C1,C9&C11
3N	-5.8	2	**A**:DC`23/H01::UNK0:O of nitro group **B**:DG`4/N2::UNK0:O of keto group	**Da5::**C2&C8 **Da6::**C8,C13&O1 **Dc21::**C7&C10 **Dg22&Dc23::**C7&C5 respectively.
3O	-5.8	4	**A**:DG`4/N3::UNK0:O of nitro group **B**: DA`5/N3:: UNK0:O of keto group **C**:DC`21/O2::UNK0:O of keto group **D**:DG`4/N2::UNK0:O of keto group	**Dg4::** C5,C6&C8 **Da6::** C9,C11, O1,&N2 **Dc21::**C9&C10 **Dg22::** C3, C5,O4&N1 **Dc21::** C9&C10 **Dc23::**C5
3P	-5.8	3	**A**: DG`12/O4:: UNK0:O of keto group **B**:DG`10/N2:: UNK0:O of nitro	**Dg10::** C11 **Dc11::**C12,O3&O4 **Dg12::**C1,C4,C5,C6,C15 &O2

Compounds	Binding affinity (kcal/mol)	Number of H-bonds with DNA	Residues involved in H-bonding	Residues involved in Hydrophobic interactions
			group C:DG`16/N2::UNK0:O of nitro group	**Dg14::** C3, C9 **Dc15::** C3 **Dg16::**C11,C7& O4 **D17::** O4
3Q	-5.9	3	A:DC`23/O3:: UNK0:O of keto group B:DG`22/N2::UNK0:O of keto group C:DG`4/N2::UNK0:O of keto group	**Dg2,Dc23,Dg24::**C1 **Dc23::**C10 **Dg22,Dc23::**C13 **Dc23::** N,C15&O1 **Dg22::** C2&C7 **Dc21::**C7 **Dg4::**C9 **Da5::**C6,C11 **Da6::**C6&C11 **Dc21::**C7,C9&C11
3R	-5.7	0	-	**Da5::** C1&C6 **Da6::** C8,C11,C13,O2&S **Dt7::** C8&O1 **Dc21::** C6,C11, C14,O1&S **Dg22::**C1

3.6. Molecular physicochemical properties and topological steric effect indexes.

Though molecular docking is a useful tool for selecting molecules with a certain structure yet it is also necessary to contemplate other theoretical tools to estimate pharmacological activity. With the available of on line software's important pharmacological properties can be taken into account. The properties includes absorption, bioavailability, permeability, blood brain barrier penetration, metabolism and excretion to achieve greater affinity for the biological receptor, lower toxicity and better scores according to [44] and the contribution of Veber et al. [45]. The molecular physicochemical properties were calculated for active compounds.

The different properties were as atom & bond count (A&BC), dreiding & MMFF94 energy, van der waals volume (VWV), van der waals surface area, (VWSA), polar surface area (PSA), number of rotatable bonds (N_B), the partition coefficient (log P), distribution coefficient (log D), donor & acceptor count (D&AC) and donor & acceptor sites (D&AS). These results demonstrate that molecular modeling and docking simulations are not sufficient for molecular screening.

In addition, by using Marvin online software topological steric effect indexes of active compounds have been calculated and are shown in energy minimized forms in Figure 7.
Lipinski's rule (Rule of Five) states that most molecules with good membrane permeability have logP <5, molecular weight <400, number of hydrogen bond acceptors <10, and number of hydrogen bond donors <5. This rule is widely used as a filter for drug-like properties. An analysis of small drug-like molecules suggests a filter of logD >0 and <3, which enhances the probability of a compound to exhibit good intestinal permeability. A poor permeation or absorption is more likely when there are more than 5 H-bond donors and 10 H-bond acceptors.

Figure 7. Energy minimized (ball and stick) models of active compounds that shows topological steric effect indexes.

The compounds (3A, 3B, 3F, 3G, 3H, 3K and 3Q), have obeyed the 'Rule of Five' with logP values <5 and HBAs ≤7. The compounds (3A, 3B, 3F, 3G, 3H, 3K and 3Q) under investigation possessed hydrogen bond donor's ≤1 and a considerable number of hydrogen bond acceptors ≤7 as shown in Table 7. The most active compounds 3A have peculiar properties with logP value equal to 2.56 and PSA equal to 71.47.

Table 7. Molecular physicochemical and topological properties of active compounds.

No.	Mol. wt	A&B C	log (P)	log (D)	No. of HBDs	No. of HBAs	PSA (2D)	Dreiding &MMFF94 Energy (kcal/mol)	VWV	VWSA (3D)	N_B
3A	239	21 & 22	2.56	1.62	1	7	71.47	53.01 & -13.37	179.43	254.96	1
3B	223	21 & 22	2.10	1.16	1	7	71.47	53.18 & -14.8	170.44	245.66	1
3F	296.6	33 & 34	4.11	4.11	0	7	62.68	81.45 & -30.63	249.84	380.45	4
3G	281.20	30 & 31	3.56	3.56	0	7	62.68	91.47 & -24.28	232.82	346.44	2
3H	265.03	30 & 31	3.20	3.20	0	7	62.68	81.55 & -31.77	240.80	371.00	3
3K	310.6	34 & 36	4.05	4.05	0	7	62.68	93.68 & -14.10	262.04	384.91	3
3Q	275.20	36 & 37	4.02	4.02	0	4	62.68	85.12 & -19.87	252.73	396.44	4

*A&BC*Atom & Bond Count,*log (P)* the Partition Coefficient, *log (D)* DistributionCoefficient*, HBDs* Number of Hydrogen Bond Donor sites, *HBAs* Number of Hydrogen Bond Acceptor sites *VWV*Van der Waals Volume, **PSA** Polar Surface Area, **VWSA** Van der Waals Surface area, , *N_B*Number of rotatable bonds obtained by Marvin sketch 6.1.3.

3.7. Solution Stability.

The solutions of the compounds (10^{-4} M) were prepared in 5% DMSO solutions of PBS at pH 7.4. The hydrolysis profiles of the compounds were assessed by recording their UV-vis. spectra after 36 h at 25°C. Water solubility is the most important and required characteristic features for good action of any drug [40, 43, 46, 47]. It was observed that all the compounds were soluble in 5% DMSO solutions of PBS at pH 7.4. All the reported compounds displayed similar spectra in PBS (5% DMSO solutions). It was observed that there was no change in UV-vis. spectra of all the compounds after 36 h indicating good stabilities of the compounds [48]. The initial and final (after 36 h of the gap) UV-vis. Spectra of 3F and 3H are shown in Figure (8a-b)UV-Vis. spectra of the compounds (coded as 3J, 3N and 3R) recorded at 0 and 36 h are shown in Figure FS3 a-c (supplementary data).
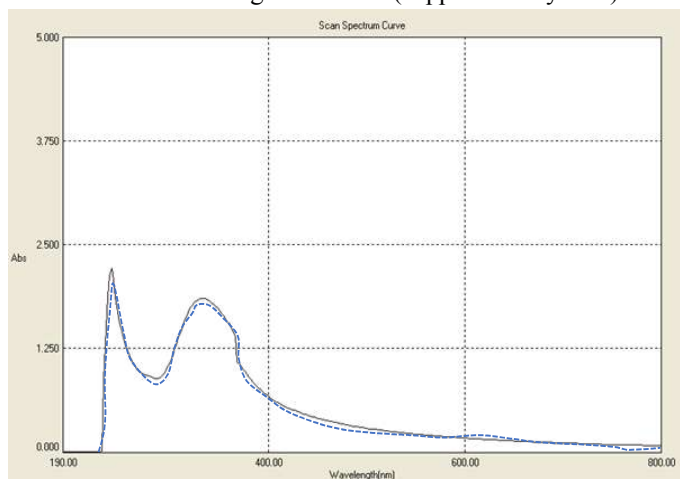
Figure 8a.UV-Vis spectra of 3F in PBS at 7.4 pH. Black solid and blue dashed lines indicate the spectra recorded at 0 and 36 h time periods, respectively.
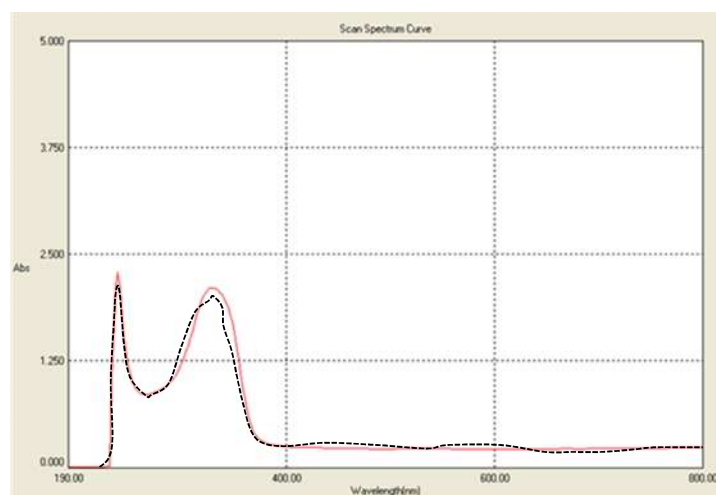
Figure 8b. UV-Vis spectra of 3H in PBS at 7.4 pH. Red solid and black dashed lines indicate the spectra recorded at 0 and 36 h time period, respectively.

3.8. Interrelationships of all studies.

As we have designed and successfully synthesized hybrid molecules of thiazolidine-2,4-diones which are capable of exhibiting anticancer activity. Among the series, few compounds (3A, 3B, 3F, 3G, 3H, 3K and 3Q) were found as most active against HepG2 cancer cell line. In this part of article, we highlight the interrelationships of all studies about active compounds which were carried out so far. The magnitude of interrelationships between different studies (Lipinski's rule, molecular docking with DNA, DNA binding and anticancer activity (human liver cancer cell line) if active compounds is shown in Figure 9. Critical analysis of data revels that all studies are in good agreements with each other.
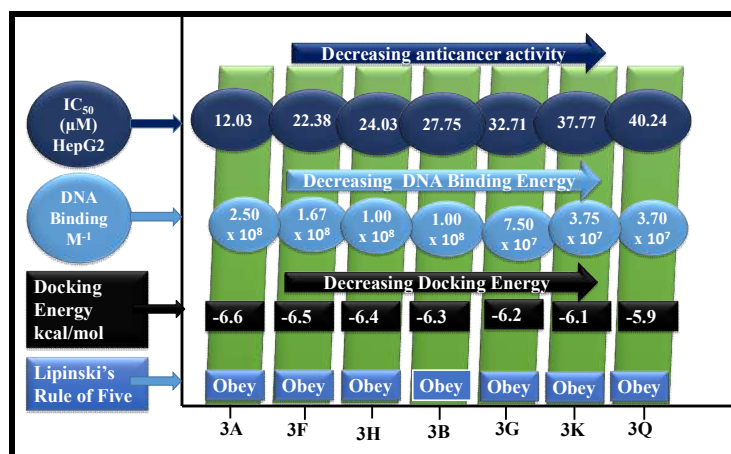
Figure 9. Correlation diagram of all studies regarding to most active compounds.

4. CONCLUSIONS

This study provided insight into the chemical and biological profiles of efficient constructed heterocyclic compounds with thiazolidine-2,4-dione moieties as cores. The cytotoxic activities of these thiazolidine-2,4-dione derivatives were evaluated against HepG2 cells. Some of the compounds displayed high cytotoxicities with IC_{50} in the range of 12 to 50 µM while some were moderately active with IC_{50} values in the range of 50 to 100 µM. These compounds indicated appreciable binding with DNA; wherein some of the compounds indicated exciting values of DNA binding (7.07×10^2-2.50×10^8 M^{-1}). Besides, some of the compounds indicated high cytotoxicities against the liver cancer cells. All the compounds (2A-3R) interacted with DNA through minor grooves. Also, the appearances of hypochromism

were the indication of binding of these compounds with DNA. DNA binding results of the compounds were also well supported by their docking studies. The docking affinities varied from 5.4 to 6.6 kcal/mol, and the compounds formed 1 to 4 hydrogen bonds with the nucleobases of DNA. Finally, 2A, 3A, 3B, 3F, 3G, 3H, 3K and 3Q were most active compounds against HepG2 cell line.

This trend of anticancer activities was well correlated with their greater interacting tendency with DNA owing to the presence of halogen atoms and two oxygen atoms in nitro group. Overall, the compounds demonstrated interesting chemico-biological features. It is warranted that their further evaluation on some other cancer cell lines will be effective.

5. REFERENCES

[1]. Chen YL., Lin SZ., Chang JY., Cheng YL., Tsai NM., Chen SP., Chang WL., Harn HJ., In vitro and in vivo studies of a novel potential anticancer agent of isochaihulactone on human lung cancer A549 cells, *Biochemical Pharmacology,* 72, 308-319, **2006.**

[2] Ferlay J., Soerjomataram I., Dikshit R., Eser S., Mathers C., Rebelo M., Parkin DM., Forman D., Bray F., Cancer incidence and mortality worldwide: sources, methods and major patterns in GLOBOCAN 2012, *International Journal of Cancer,* 136, E359-E386, **2015.**

[3] Ali I., Wani WA., Haque A., Saleem K., Glutamic acid and its derivatives: candidates for rational design of anticancer drugs, *Future Medicinal Chemistry,* 5, 961-978, **2013.**

[4] Ali I., Haque A., Saleem K., Hsieh MF., Curcumin-I Knoevenagel's condensates and their Schiff's bases as anticancer agents: Synthesis, pharmacological and simulation studies, *Bioorganic Medicinal Chemistry,* 21, 3808-3820, **2013.**

[5] Ali I., Lone MN., Al-Othman Z., Al-Warthan A., Heterocyclic Scaffolds: Centrality in Anticancer Drug Development, *Current Drug Targets,* 16, 711-734, **2015.**

[6] Verma A., Saraf SK., 4-Thiazolidinone – A biologically active scaffold, *European Journal of Medicinal Chemistry,* 43, 897-905, **2008.**

[7] Andres CJ., Bronson JJ., D'Andrea SV., Deshpande MS., Falk PJ., Grant-Young KA., Harte WE., Ho H-T., Misco PF., Robertson JG., 4-Thiazolidinones: novel inhibitors of the bacterial enzyme murB. *Bioorganic Medicinal Chemistry Letters,* 10, 715-717, **2000.**

[8] Tuncbilek M., Altanlar N., Synthesis of New 3-(Substituted Phenacyl)-5-[3′-(4H-4-oxo-1-benzopyran-2-yl)-benzylidene]-2,4-thiazolidinediones and their Antimicrobial Activity, *Arch der Pharmazie,* 339, 213-216, **2006.**

[9] Devinyak O., Havrylyuk D., Zimenkovsky B., Lesyk R., Computational Search for Possible Mechanisms of 4-Thiazolidinones

Anticancer Activity: The Power of Visualization, *Molecular Informatics,* 33, 3, 216-229, **2014.**

[10] Liu K., Rao W., Parikh H., Li Q., Guo TL., Grant S., Kellogg GE., Zhang S.,. 3,5-Disubstituted-thiazolidine-2,4-dione analogs as anticancer agents: Design, synthesis and biological characterization, *European Journal of Medicinal Chemistry,* 47, 125-137, **2012.**

[11] Salamone S., Colin C., Grillier-Vuissoz I., Kuntz S., Mazerbourg S., Flament S., Martin H., Richert L., Chapleur Y., Boisbrun M., Synthesis of new troglitazone derivatives: anti-proliferative activity in breast cancer cell lines and preliminary toxicological study, *European Journal of Medicinal Chemistry,* 51, 206-215, **2012.**

[12] Alegaon SG., Alagawadi KR., New thiazolidine-2, 4-diones as antimicrobial and cytotoxic agent, *Medicinal Chemistry Research,* 21, 3214-3223, **2012.**

[13] Chen EM., Lu PJ., Shawc AY., Synthesis and Antiproliferative Evaluation of 2 0- Arenesulfonyloxy-5-benzylidene-thiazolidine-2, 4-diones, *Journal of Heterocyclic Chemistry,* 49, 792-798, **2012.**

[14] Welsch ME., Snyder SA., Stockwell BR., Privileged scaffolds for library design and drug discovery, *Current Opinion Chemical Biology,* 14, 347-361, **2010.**

[15] Zhang C., Moran EJ., Woiwode TF., Short KM., Mjalli AM., Synthesis of tetrasubstituted imidazoles via α-(N-acyl-N-alkylamino)-β-ketoamides on Wang resin, *Tetrahedron Letters,* 37, 751-754, **1996.**

[16] Knight SD., Adams ND., Burgess JL., Chaudhari AM., Darcy MG., Donatelli CA., Luengo JI., Newlander KA., Parrish CA., Ridgers LH., Discovery of GSK2126458, a highly potent inhibitor of PI3K and the mammalian target of rapamycin, ACS Medicinal Chemistry Letters, 1, 39-43, **2010.**

[17] Liu K., Guo TL., Hait NC., Allegood J., Parikh HI., Xu W., Kellogg GE., Grant S., Spiegel S., Zhang S., Biological characterization of 3-(2-amino-ethyl)-5-[3-(4-butoxyl-phenyl)-propylidene]-thiazolidine-2,   4-

dione (K145) as a selective sphingosine kinase-2 inhibitor and anticancer agent, PloS one, 8, e56471, **2013.**

[18] Li Q., Al-Ayoubi A., Guo T., Zheng H., Sarkar A., Nguyen T., Eblen ST., Grant S., Kellogg GE., Zhang S.,. Structure–activity relationship (SAR) studies of 3-(2-amino-ethyl)-5-(4-ethoxy-benzylidene)-thiazolidine-2, 4-dione: Development of potential substrate-specific ERK1/2 inhibitors, *Bioorganic Medicinal Chemistry Letters*, 19, 6042-6046, **2009.**

[19] Mohsen A., Omar M., Salama H., Eshba N., Novel thiazolidine-2, 4-dione-4-thiosemicarbazone and 4-[(3, 4-diaryl-3H-thiazol-2-yl) azo] thiazolidin-2-one derivatives: synthesis and evaluation for antimicrobial and anticancer properties, *Il Farmaco; edizione scientifica,* 40, 49-57, **1985.**

[20] Bruker Molecular Analysis Research Tool. Bruker AXS, Madison, Wisconsin (USA), **2016.**

[21] Sheldrick G 2001. SAINT-NT, version 6.04. Bruker Analytical X-ray Systems: Madison, WI, **2016.**

[22] Sheldrick G: SHELXTL-NT, version 6.10, Bruker Analytical X-ray Systems, Madison, WI, 2000;(d) B. Klaus, DIAMOND, version, 2, **2016.**

[23] Macrae CF, Edgington PR, McCabe P, Pidcock E, Shields GP, Taylor R, Towler M, Streek Jvd 2006. Mercury: visualization and analysis of crystal structures. J Appl Crystal, 39, 453-457, **2006.**

[24] Wani WA., Al-Othman Z., Ali I., Saleem K., Hsieh MF., Copper (II), nickel (II), and ruthenium (III) complexes of an oxopyrrolidine-based heterocyclic ligand as anticancer agents, *Journal of Coordination Chemistry*, 67, 2110-2130, **2014.**

[25] Ali I., Wani WA., Saleem K., Hsieh M-F., Anticancer metallodrugs of glutamic acid sulphonamides: in silico, DNA binding, hemolysis and anticancer studies, *RSC Advances*, 4, 29629-2964, **2014.**

[26] Shahabadi N., Kashanian S., Purfoulad M.,. DNA interaction studies of a platinum (II) complex, PtCl 2 (NN)(NN= 4, 7-dimethyl-1, 10-phenanthroline), using different instrumental methods, *Spectrochim Acta Mol Biomol Spectroscopy*, 72, 757-761, **2009.**

[27] Allardyce CS., Dyson PJ., Ellis DJ., Heath SL., [Ru (η6-p-cymene) Cl2 (pta)](pta= 1, 3, 5-triaza-7-phosphatricyclo-[3.3. 1.1] decane): a water soluble compound that exhibits pH dependent DNA binding providing selectivity for diseased cells, *Chemical Communications*, 15, 1396-1397, **2001.**

[28] Sanner MF., Python: a programming language for software integration and development, *Journal of Molecular Graphics and Modelling*, 17, 57-61, **1999.**

[29] http://www.rcsb.org/pdb/explore/explore.do?structureId=1bna

[30] Drew HR., Wing RM., Takano T., Broka C., Tanaka S., Itakura K., Dickerson RE., Structure of a B-DNA dodecamer: conformation and dynamics, *Proceedings of the National Academy of Sciences of the United States of America,* 78, 2179-2183, **1981.**

[31] Morris GM., Goodsell DS., Halliday RS., Huey R., Hart WE., Belew RK., Olson AJ., Automated docking using a Lamarckian genetic algorithm and an empirical binding free energy function, *Journal of Computational Chemistry*, 19, 1639-1662, **1998.**

[32] Huey R., Morris GM., Olson AJ., Goodsell DS., A semiempirical free energy force field with charge-based desolvation, *Journal of Computational Chemistry,* 28, 1145-1152, **2007.**

[33] Trott O., Olson AJ.,. AutoDock Vina: improving the speed and accuracy of docking with a new scoring function, efficient optimization, and multithreading, *Journal of Computational Chemistry,* 31, 455-461, **2010.**

[34] Ali I., Wani WA., Saleem K., Hseih M-F., Design and synthesis of thalidomide based dithiocarbamate Cu (II), Ni (II) and Ru (III) complexes as anticancer agents, *Polyhedron,* 56, 134-143, **2013.**

[35] Shahabadi N., Kashanian S., Mahdavi M., Sourinejad N., DNA interaction and DNA cleavage studies of a new platinum (II) complex containing aliphatic and aromatic dinitrogen ligands, *Bioinorganic Chemistry and Applications*, **2011.**

[36] Erkkila KE., Odom DT., Barton JK., Recognition and reaction of metallointercalators with DNA, *Chemical Reviews*, 99, 2777-2796, **1999.**

[37] Chen LM., Liu J., Chen JC., Tan CP., Shi S., Zheng K-C., Ji LN., Synthesis, characterization, DNA-binding and spectral properties of complexes [Ru (L) 4 (dppz)] 2+(L= Im and MeIm), *Journal of Inorganic Biochemistry,* 102, 330-341, **2008.**

[38] Pasternack RF., Gibbs EJ., Villafranca JJ., Interactions of porphyrins with nucleic acids, *Biochemistry*, 22, 5409-5417, **1983.**

[39] Zhao P., Xu LC., Huang JW., Liu J., Yu HC., Zheng KC., Ji LN., Experimental and DFT studies on DNA binding and photocleavage of two cationic porphyrins: effects of the introduction of a carboxyphenyl into pyridinium porphyrin, Spectrochimica Acta Molecular Biomolecular Spectroscopy, 71, 1216-1223, **2008.**

[40] Arjmand F., Aziz M., Chauhan M.,. Synthesis, spectroscopic studies of new water-soluble Co (II) and Cu (II) macrocyclic complexes of 4, 15-bis (2-hydroxyethyl)-2, 4, 6, 13, 15, 17-hexaazatricyclodocosane: their interaction studies with calf thymus DNA and guanosine 5′ monophosphate, *Journal of Inclusion Phenomena and Macrocyclic Chemistry*, 61, 265-278, **2008.**

[41] Sun Y., Zhang H., Bi S., Zhou X., Wang L., Yan Y., Studies on the arctiin and its interaction with DNA by spectral methods, *Journal of Luminescence,* 131, 2299-2306, **2011.**

[42] Küng A., Pieper T., Wissiack R., Rosenberg E., Keppler BK., Hydrolysis of the tumor-inhibiting ruthenium (III) complexes HIm trans-[RuCl4 (im) 2] and HInd trans-[RuCl4 (ind) 2] investigated by means of HPCE and HPLC-MS, JBIC 6, 292-299, **2001.**

[43] Bacac M., Hotze AC., van der Schilden K., Haasnoot JG., Pacor S., Alessio E., Sava G., Reedijk J., The hydrolysis of the anti-cancer ruthenium complex NAMI-A affects its DNA binding and antimetastatic activity: an NMR evaluation, *Journal of Inorganic Biochemistry*, 98, 402-412, **2004.**

[44] Lipinski's Rules Lipinski CA., Lombardo F., Dominy BW., Feeney PJ., Experimental and computational approaches to estimate solubility and permeability in drug discovery and development settings, *Advanced Drug Delivery Reviews*, 64, 4-17, **2012.**

[45] Veber DF., Johnson SR., Cheng H-Y., Smith BR., Ward KW., Kopple KD., Molecular properties that influence the oral bioavailability of drug candidates, *Journal of Medicinal Chemistry*, 45, 2615-2623, **2002.**

[46] Tan C., Hu S., Liu J., Ji L.,. Synthesis, characterization, antiproliferative and anti-metastatic properties of two ruthenium–DMSO complexes containing 2, 2′-biimidazole, *European Journal of Medicial Chemistry,* 46, 1555-1563, **2011.**

[47] Büchel GE., Stepanenko IN., Hejl M., Jakupec MA., Keppler BK., Arion VB.,. En route to osmium analogues of KP1019: Synthesis, structure, spectroscopic properties and antiproliferative activity of trans-[OsIVCl4 (Hazole) 2], *Inorganic Chemistry*, 50, 7690, **2011.**

[48] Giovagnini L., Sitran S., Montopoli M., Caparrotta L., Corsini M., Rosani C., Zanello P., Dou QP., Fregona D.,. Chemical and biological profiles of novel copper (II) complexes containing S-donor ligands for the treatment of cancer, *Inorganic Chemistry,* 47, 6336-6343, **2008.**

6. ACKNOWLEDGEMENTS

Conflict of Interest

The authors claim no conflict of interest.

Supplementary Data

Table TS1. UV-Vis data for compounds (3A-3R). Wavelength and Hypochromic shifts on increasing DNA concentrations of DNA (0.3×10^{-5}M -1.7 $\times 10^{-5}$M).

S. No.	Compounds	λ_{max}free (nm)	λ_{max}bound (nm)	$\Delta\lambda_{max}$(nm)	Abs free	Abs bound	ΔAbs
1	**3A**	336	337	1	1.421	0.775	0.646
2	**3B**	330	332	2	2.211	1.276	0.935
3	**3C**	344	335	1	1.371	0.740	0.631
4	**3D**	362	366	4	1.168	0.921	0.247
5	**3E**	338	339	1	0.520	0.145	0.376
6	**3F**	336	338	2	0.278	0.127	0.151
7	**3G**	350	352	2	0.286	0.268	0.018
8	**3H**	322	332	10	1.978	1.703	0.275
9	**3I**	330	331	1	0.208	0.148	0.06
10	**3J**	330	331	1`	0.745	0.213	0.532
11	**3K**	334	338	4	1.499	0.135	1.364
12	**3L**	348	350	2	0.692	0.342	0.35
13	**3M**	334	336	2	1.676	0.795	0.881
14	**3N**	354	366	12	1.486	0.858	0.628
15	**3O**	348	349	1	0.642	0.289	0.353
16	**3P**	330	332	2	1.019	0.185	0.834
17	**3R**	250	264	14	2.067	1.167	0.100
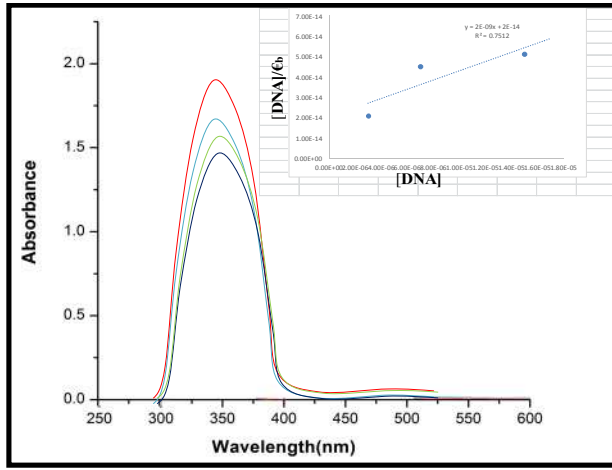
(a): 3B
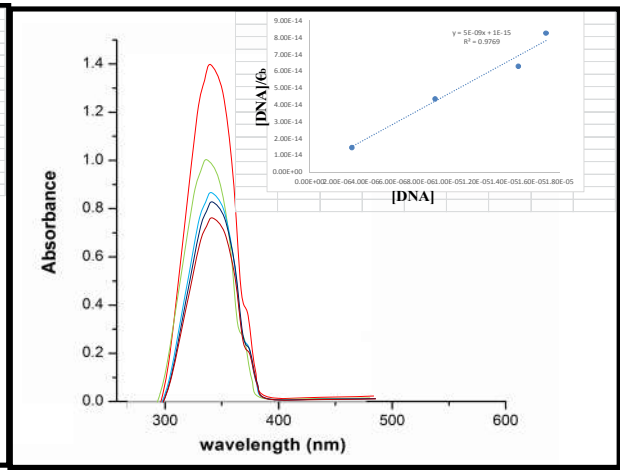
(b): 3C
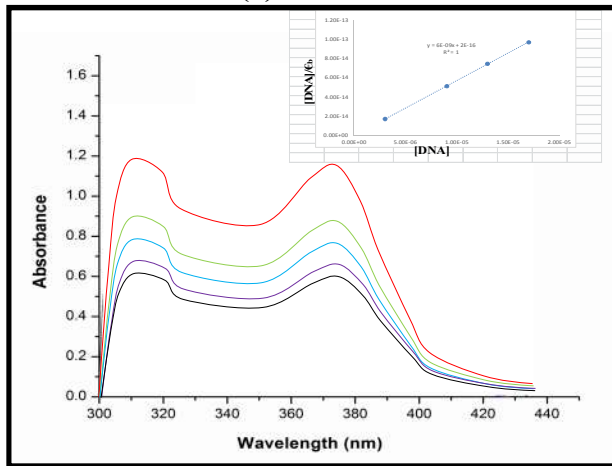
(c): 3D

(d): 3E

(e): 3G

(f): 3H

(g): 3I

(h): 3J

(i): 3K

(j): 3L

(k): 3N

(l): 3O

(m): 3P

(n): 3R
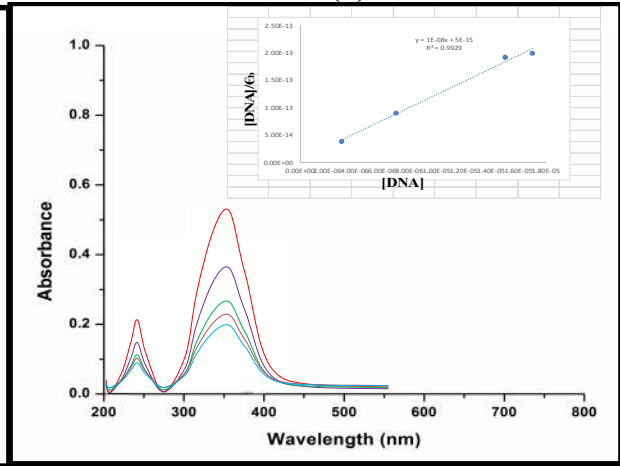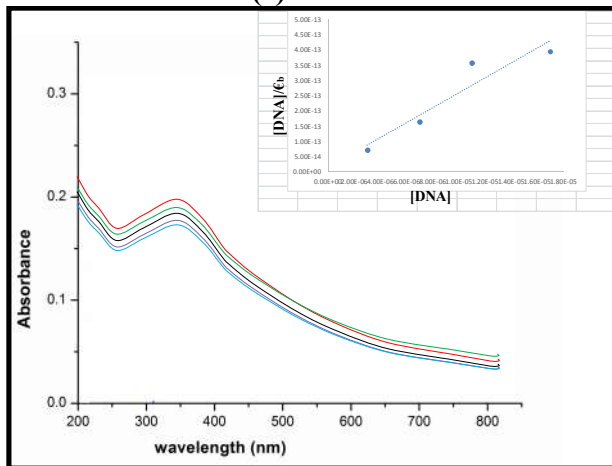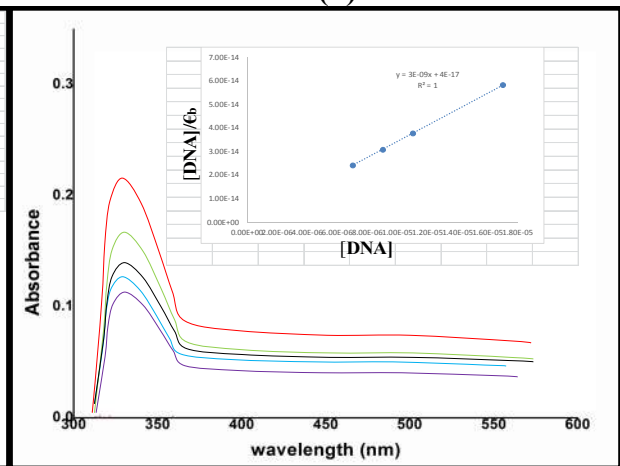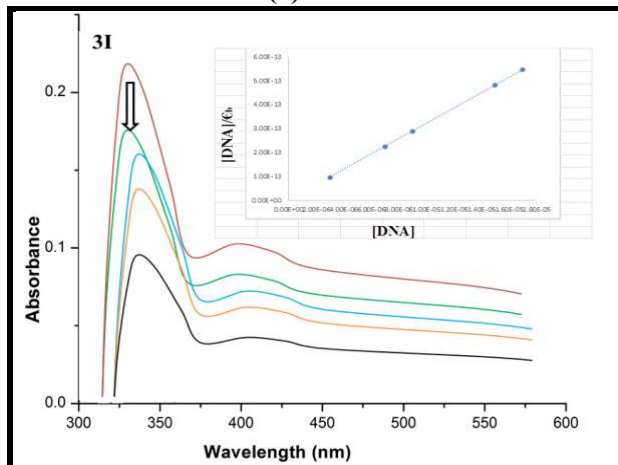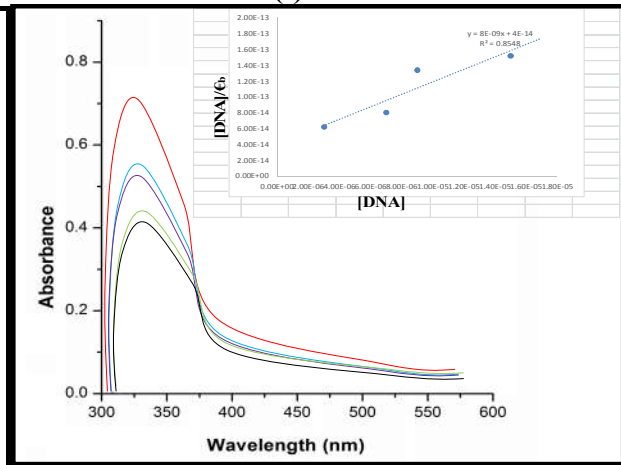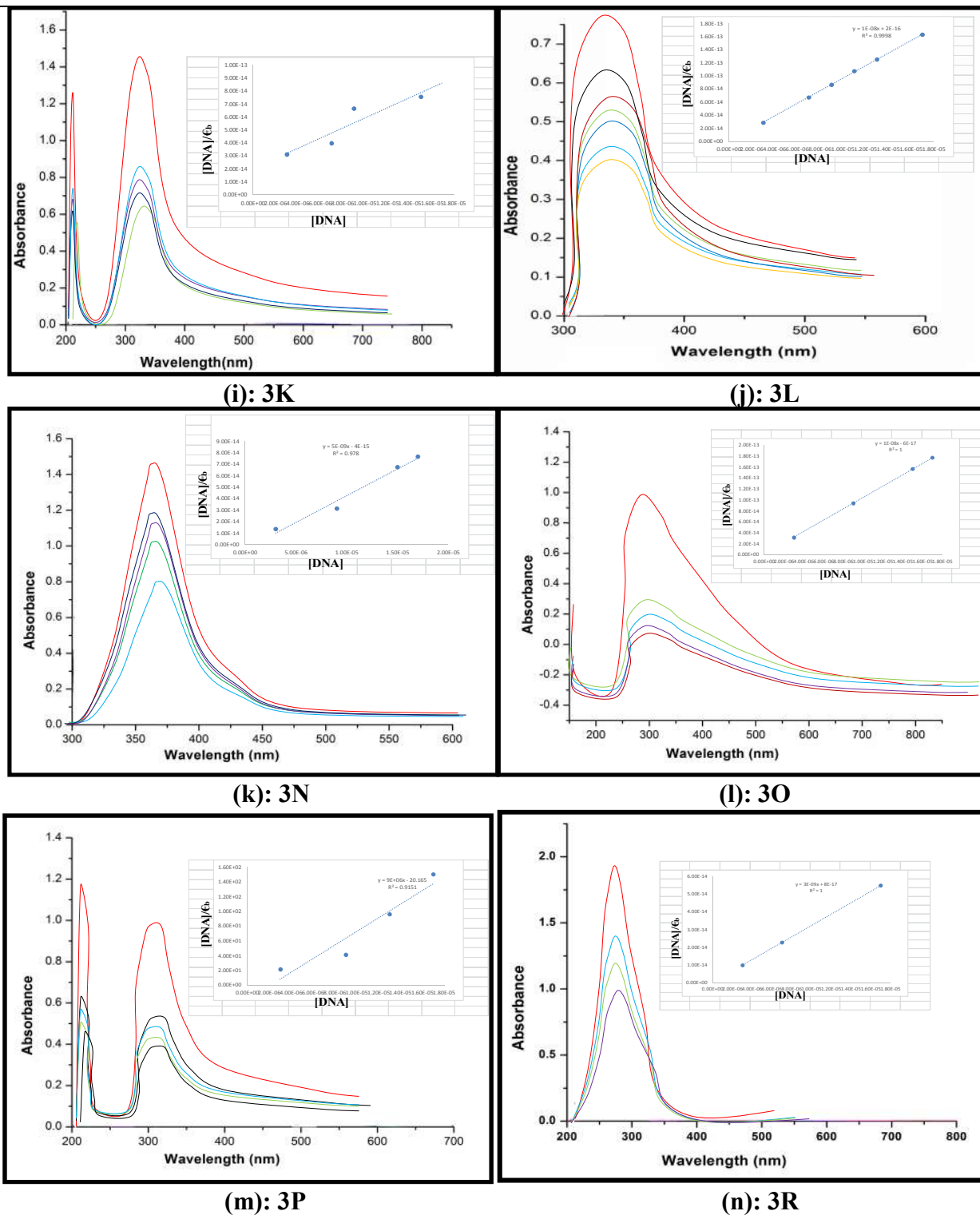
Figure FS1 (a-n). Absorption spectra of **3B-3R** (0.2×10^{-7} M) in in the absence (red line) and presence (other coloured lines) of increasing DNA concentrations; 0.3×10^{-5}M -1.7×10^{-5}M respectively. Arrow indicates the hypochromic shifts on increasing DNA concentrations. Inset: plots of [DNA]/ϵb (M2cm-1) versus [DNA] for the titration of Ct-DNA with compounds.
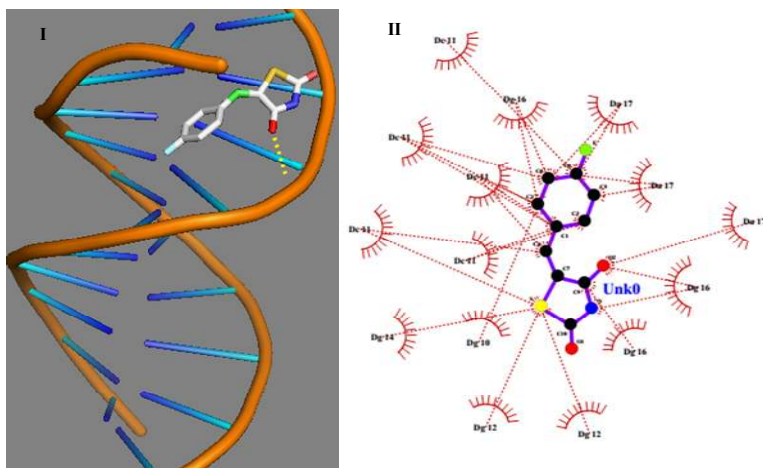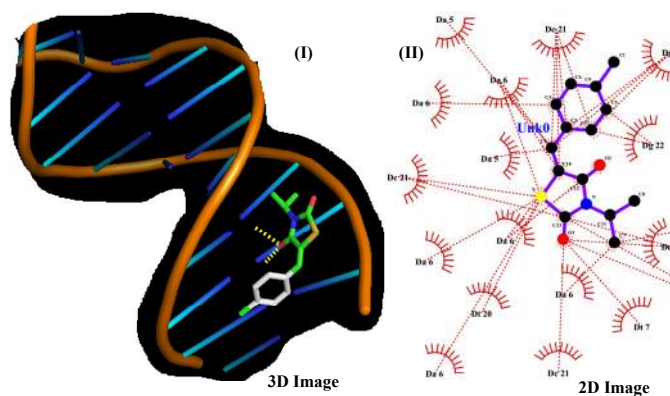
Figure FS2a. 3D- and 2D-docking images of 3B with DNA. Image (I) indicate the interaction of 3B with DNA *via* minor groove, and image (II) indicates the interaction is mainly through hydrophobic attractions.
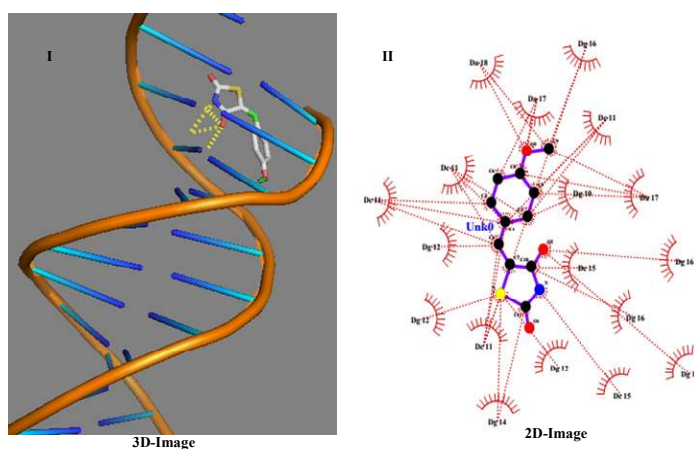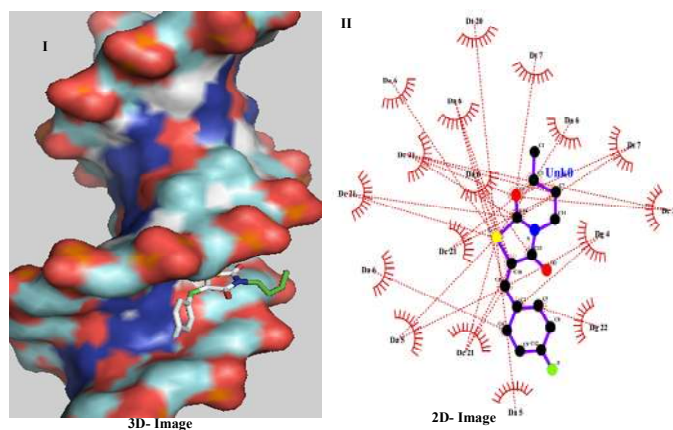

Figure FS2b. 3D- and 2D- docking images of 3C with DNA. Image (I) indicate the interaction of 3C with DNA *via* minor groove, and image (II) indicates the interaction is mainly through hydrophobic attractions.
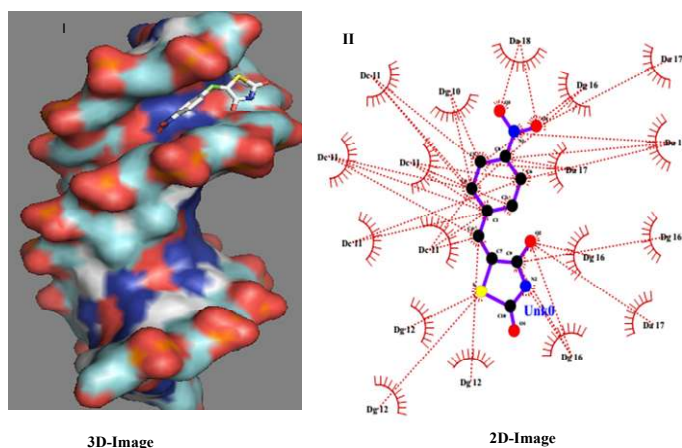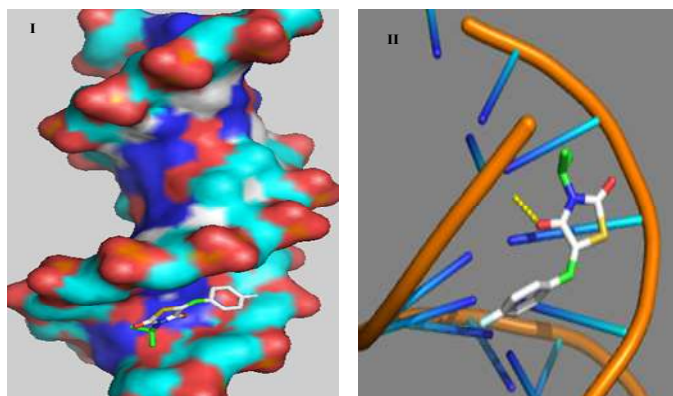

Figure FS2c. 3D- and 2D- docking images of 3D with DNA. Image (I) indicate the interaction of 3D with DNA *via* minor groove, and image (II) indicates the interaction is mainly through hydrophobic attractions.
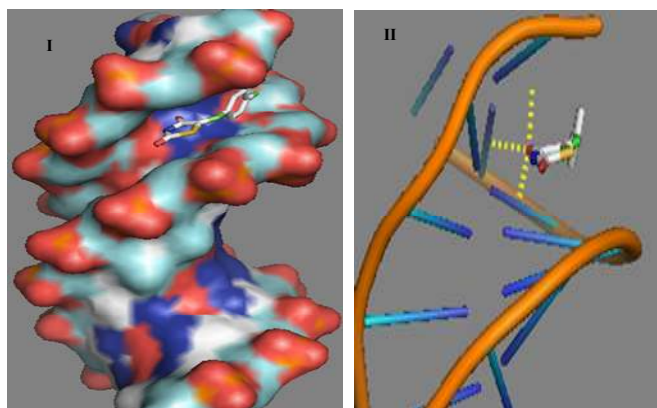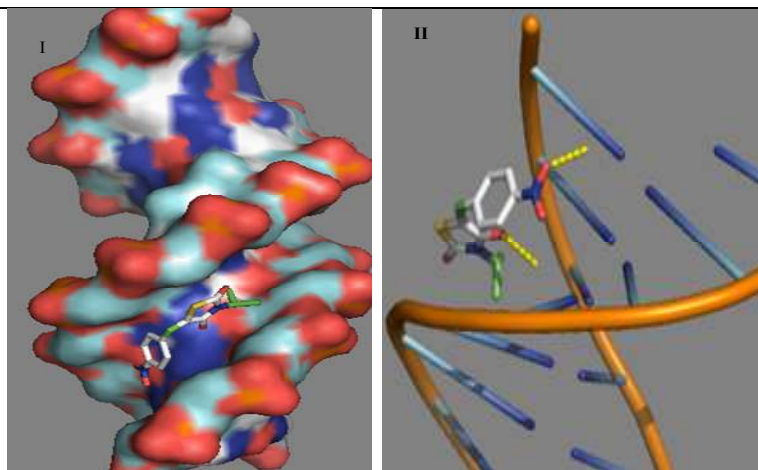
Figure FS2d. 3D- docking images of 3E with DNA. Image (I) indicate the interaction of 3E with DNA *via* minor groove, and image (II) indicates the polar attractions.

Figure FS2e. 3D and 2D- docking images of 3F with DNA. Image (I) indicate the interaction of 3F with DNA *via* minor groove, and image (II) indicates the interaction is mainly through hydrophobic attractions.

Figure FS2f.3D- and 2D- docking images of **3H** with DNA. Image (I) indicate the interaction of **3H** with DNA *via* minor groove, and image (II) indicates the interaction is mainly through hydrophobic attractions.
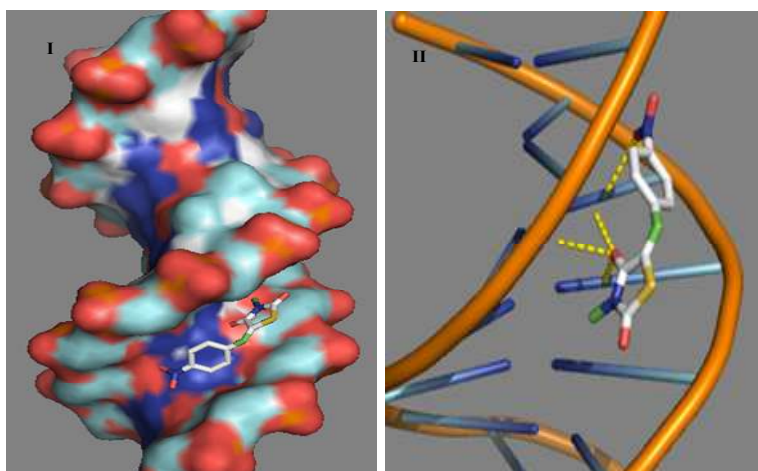
Figure FS2g. 3D- docking images of 3Iwith DNA. Image (I) indicate the interaction of 3I with DNA *via* minor groove, and image (II) indicates the polar attractions.
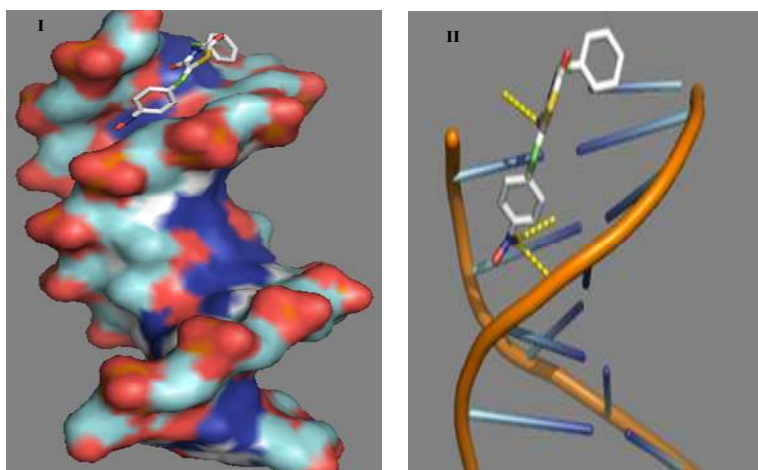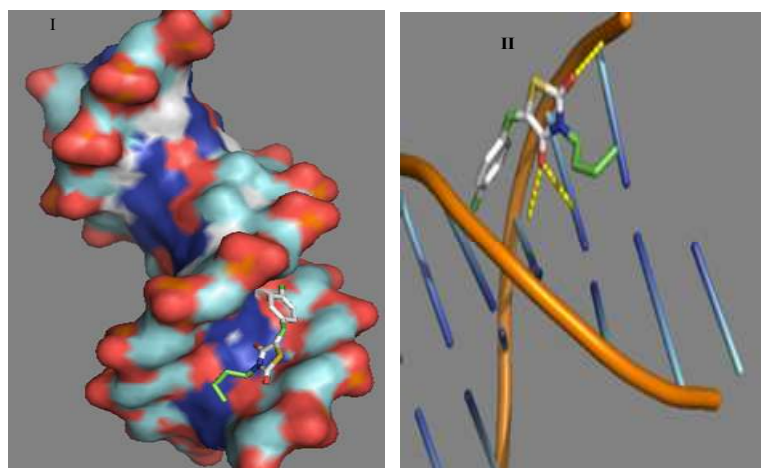

3D- Image   **2D- Image**

Figure FS2h. 3D- and 2D- docking images of 3J with DNA. Image (I) indicate the interaction of 3J with DNA *via* minor groove, and image (II) indicates the interaction is mainly through hydrophobic attractions.

3D-Image   **2D-Image**

Figure FS2i. 3D- and 2D- docking images of 3L with DNA. Image (I) indicate the interaction of 3L with DNA *via* minor groove, and image (II) indicates the interaction is mainly through hydrophobic attractions.

3D-Image   **2D-Image**

Figure FS2j. 3D- and 2D- docking images of 3M with DNA. Image (I) indicate the interaction of 3M with DNA *via* minor groove, and image (II) indicates the interaction is mainly through hydrophobic attractions.

Figure FS2k. 3D- docking images of 3N with DNA. Image (I) indicate the interaction of 3N with DNA *via* minor groove, and image (II) indicates polar attractions.

Figure FS2l. 3D- docking images of 3O with DNA. Image (I) indicate the interaction of 3O with DNA *via* minor groove, and image (II) indicates the polar attractions.
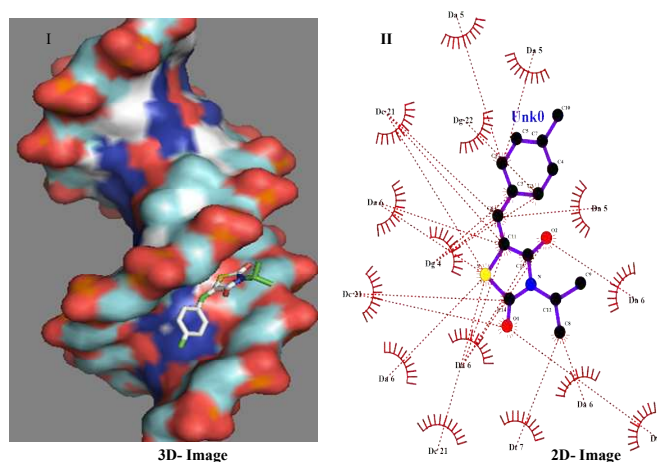

Figure FS2m. 3D- docking images of 3P with DNA. Image (I) indicate the interaction of 3P with DNA *via* minor groove, and image (II) indicates the polar attractions.

Figure FS2n. 3D- docking images of **3Q** with DNA. Image (I) indicate the interaction of **3Q** with DNA *via* minor groove, and image (II) indicates the polar attractions.

Figure FS2o. 3D- and 2D- docking images of 3R with DNA. Image (I) indicate the interaction of 3R with DNA *via* minor groove, and image (II) indicates the interaction is mainly through hydrophobic attractions.
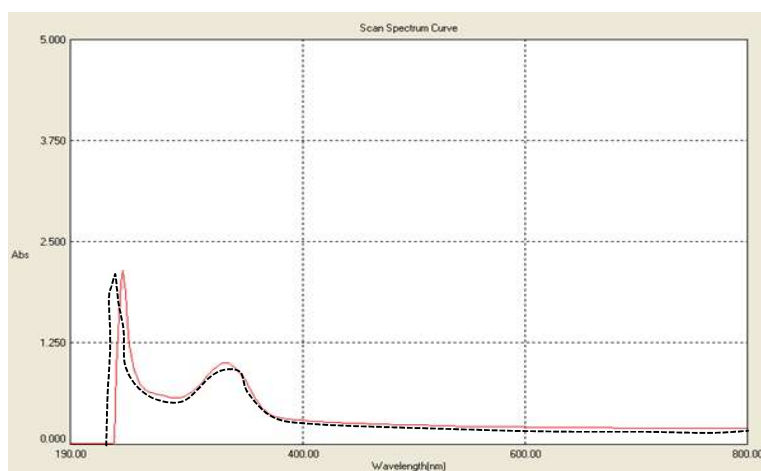
Figure FS3a. UV-Vis spectra of 3J in PBS at 7.4 pH. Red solid and black dashed line indicates the spectra recorded at 0 and 36 h time periods, respectively.
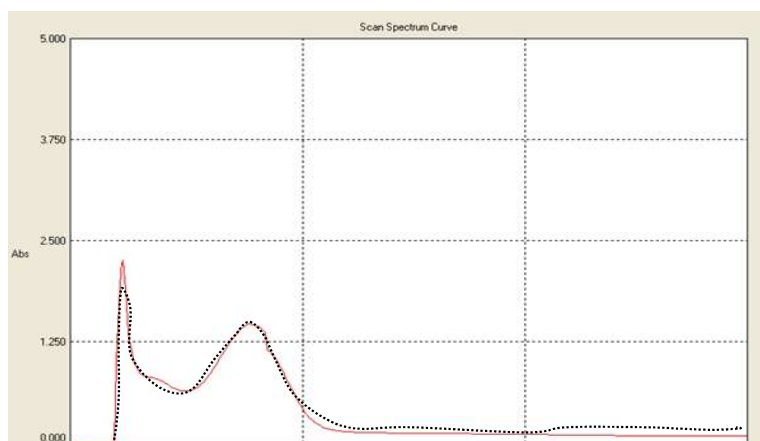
Figure **FS3b.** UV-Vis spectra of **3N** in PBS at 7.4 pH. Red solid and black dashed line indicated the spectra recorded at 0 and 36 h time periods, respectively.
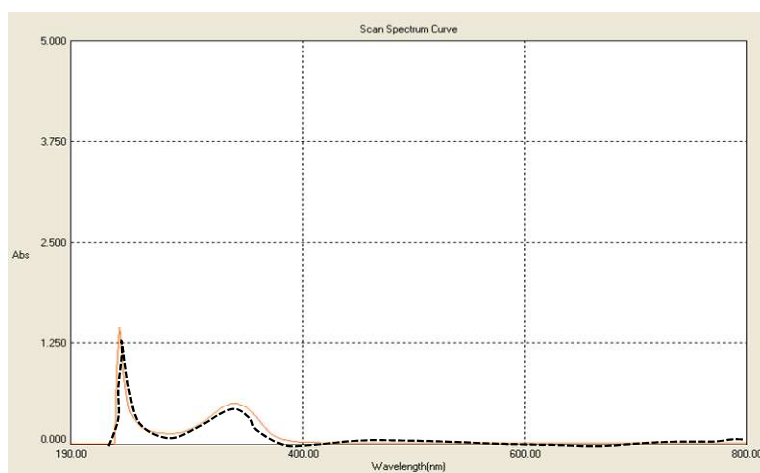

Figure FS3c. UV-Vis spectra of 3R in PBS at 7.4 pH. Red solid and black dashed line indicated the spectra recorded at 0 and 36 h time periods, respectively.